# ENRICO FERMI ATOMIC POWER PLANT

## NUCLEAR TEST SERIES

## POWER COEFFICIENT MEASUREMENTS FOR THE ENRICO FERMI REACTOR

R. E. Mueller

H. A. Wilber*



*Presently with Power Reactor Development Company

November, 1967

ATOMIC POWER
DEVELOPMENT ASSOCIATES, INC.

## DISCLAIMER

## FOREWORD

This report is one of a series of reports on the low-power (up to 1 Mwt) and high-power (up to 100 Mwt) nuclear testing of the Enrico Fermi fast breeder reactor. The Nuclear Test Program is planned, directed, and evaluated by Atomic Power Development Associates, Inc. (APDA). The tests are conducted by Power Reactor Development Company (PRDC), who own and operate the reactor proper. The steam generators and electrical generation facilities are owned by The Detroit Edison Company (DECo).

Many people have contributed to the success of the nuclear testing of the Enrico Fermi reactor. Listed below are the names of those people, exclusive of the authors, who made significant contributions to some phase of the work reported in this document.

| APDA | PRDC | DECo |
|---|---|---|
| H. J. Allgeier | E. L. Alexanderson | F. J. Locke |
| C. E. Branyan | D. Doiron | |
| R. C. Callen | W. R. Olson | |
| A. E. Klickman | G. Yax | |
| J. B. Nims | | |
| E. M. Page | | |

# TABLE OF CONTENTS

TABLE OF CONTENTS (Con't)

## LIST OF ILLUSTRATIONS

## LIST OF TABLES

## SUMMARY

Power coefficient measurements for the Enrico Fermi reactor were made by static physics measurements at four different times during the high-power nuclear test program. The measurements were made at increasing maximum power levels ranging from 13 Mwt to 100 Mwt nominal power in the period from January 13, 1966 through July 12, 1966. Two of the measurements were made at two-thirds nominal Core A flow and two at full Core A flow. The measurements at each power level were made during both power ascent and power decent to investigate possible hysteresis effects such as have been seen in EBR-II.

The results of the power coefficient measurements, after all corrections were made, were as follows:

| Power Range | ¢/Mwt |
|---|---|
| 0 to 13 Mwt, 2/3 flow | -0.247 ±13% |
| 0 to 20 Mwt, full flow | -0.204 ±13% |
| 0 to 67 Mwt, 2/3 flow | -0.263 ±7% |
| 0 to 100 Mwt, full flow | -0.174 ±7% |

No hysteresis effect was seen in any of the power coefficient measurements.

The measured power coefficient values appear to be consistent among themselves within the experimental error limits, except the 0 to 20 Mwt full flow value. No explanation has been found for its inconsistency.

The values obtained indicate that the feedback reactivity is approximately 28 per cent smaller than originally calculated (excluding the 20 Mwt results). This result is supported by dynamic oscillator analysis. A smaller power coefficient value was expected, because the earlier measured isothermal temperature coefficient was also found to be smaller than predicted, although by only 12 per cent. Nevertheless, power coefficient agreement to within 28 per cent of the calculated value is considered adequate, since the value of the power coefficient depends on a combination of several complex effects not present in the isothermal temperature coefficient.

The power coefficient data at different flows were also analyzed to obtain an estimate of the flow coefficient. These results showed that only four per cent of the feedback was flow-independent. This is considerably less than was anticipated, but the results have a relatively large uncertainty.

In an attempt to explain the observed discrepancies, a review of the original power coefficient calculations was made. Taken into account were the experimentally determined fuel and coolant worth data obtained in the low-power test program and various reactor design modifications which have been made since the time of the original power coefficient calculations. The new calculations appear to adequately explain the difference between measured and predicted coefficients.

# I. PURPOSE OF TEST

The purpose of this test was to determine periodically, by means of static physics measurements, the power coefficient of reactivity ($\Delta k/k/Mwt$) in the Enrico Fermi reactor at different power levels and primary flow rates during the step-by-step power escalation program followed in the approach to full power. These data were used in the kinetic analyses of the reactor to verify compliance with the technical specifications, to determine the reactivity override required to operate the reactor at full power, and to determine the flow effect on reactivity in the reactor. They were also used to determine whether there was any variation in the power coefficient as a function of power, whether it changed with time, and whether a hysteresis effect existed similar to that seen in EBR-II, where a different power coefficient value was sometimes measured during power ascent and power descent.

# II. DESCRIPTION OF THE ENRICO FERMI REACTOR AND ITS POWER REACTIVITY EFFECTS

## A. GENERAL DESCRIPTION

The Enrico Fermi reactor and its associated structures are shown in perspective in Figure 1. The reactor is contained in a stainless steel vessel sealed at the top by a rotating shield plug which supports the control mechanisms, the fuel subassembly holddown mechanism, and the subassembly handling mechanism. The reactor is of the fast breeder type, cooled by sodium and operated at essentially atmospheric pressure. The maximum reactor power possible with the first core loading (Core A) is 200 Mwt; however, the Nuclear Test Program was terminated when the reactor achieved 100 Mwt, a power level which is considered sufficient for the planned use of the Fermi reactor as a test facility.

The reactor core and blanket are located in the lower reactor vessel and consist of 2.646-inch-square subassemblies containing the fuel pins and blanket rods. The core and blanket subassemblies are arranged to approximate a cylinder about 80 inches in diameter and 70 inches high. The core, which is contained in the central portion of the core subassemblies, approximates a right cylinder 31 inches in diameter and 31 inches high; it is axially and radially surrounded by breeder blankets. The fuel in the first core loading consists of zirconium-clad pins, 0.158 inch in diameter, containing U-10 w/o molybdenum alloy in which the uranium is enriched to 25.6 w/o in U-235. Each fuel subassembly in the core contains 140 fuel pins for a total mass of approximately 4.75 kilograms of U-235 per subassembly. The inner and outer radial blanket subassemblies each contain twenty-five 0.443-inch-diameter blanket rods of depleated U-3 w/o molybdenum alloy.

The reactor cross section, shown in Figure 2, indicates the placement of individual components within the lower reactor vessel. There is a total of 149 central lattice positions that are occupied by core and inner radial blanket subassemblies, the antimony-beryllium (Sb-Be) neutron source, and 10 operating control and safety rod channels. All of these positions are supplied with sodium coolant flowing upward from a high-pressure plenum which is connected to the discharge lines of the three primary sodium pumps. The coolant flows upward through the individual core and inner radial blanket subassemblies and into a large upper plenum. From there, it flows by gravity to the three intermediate heat exchangers and then to the suction side of the primary pumps. Sodium also is used in the secondary cooling system.

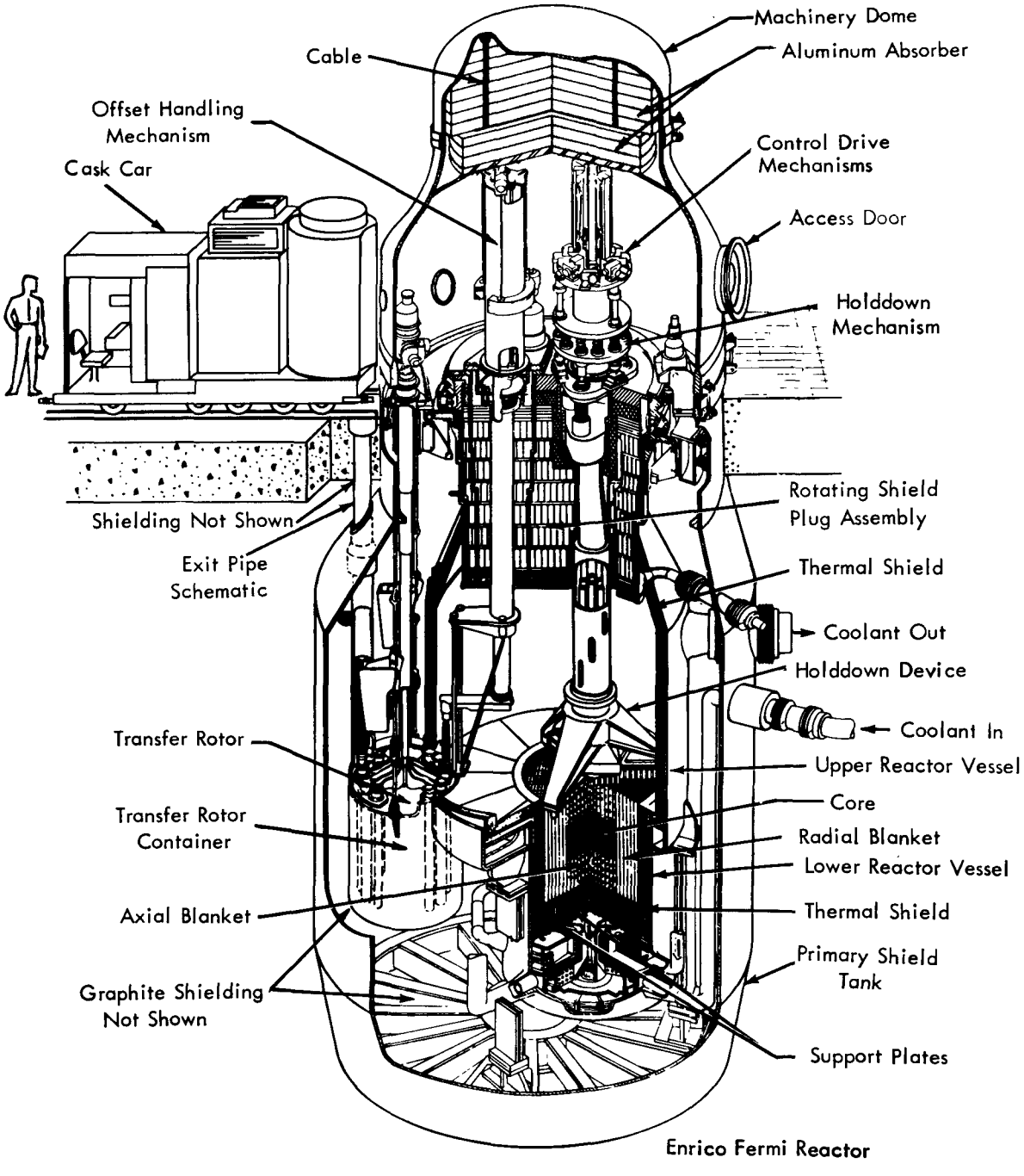


**FIG. 1 PERSPECTIVE VIEW OF REACTOR**

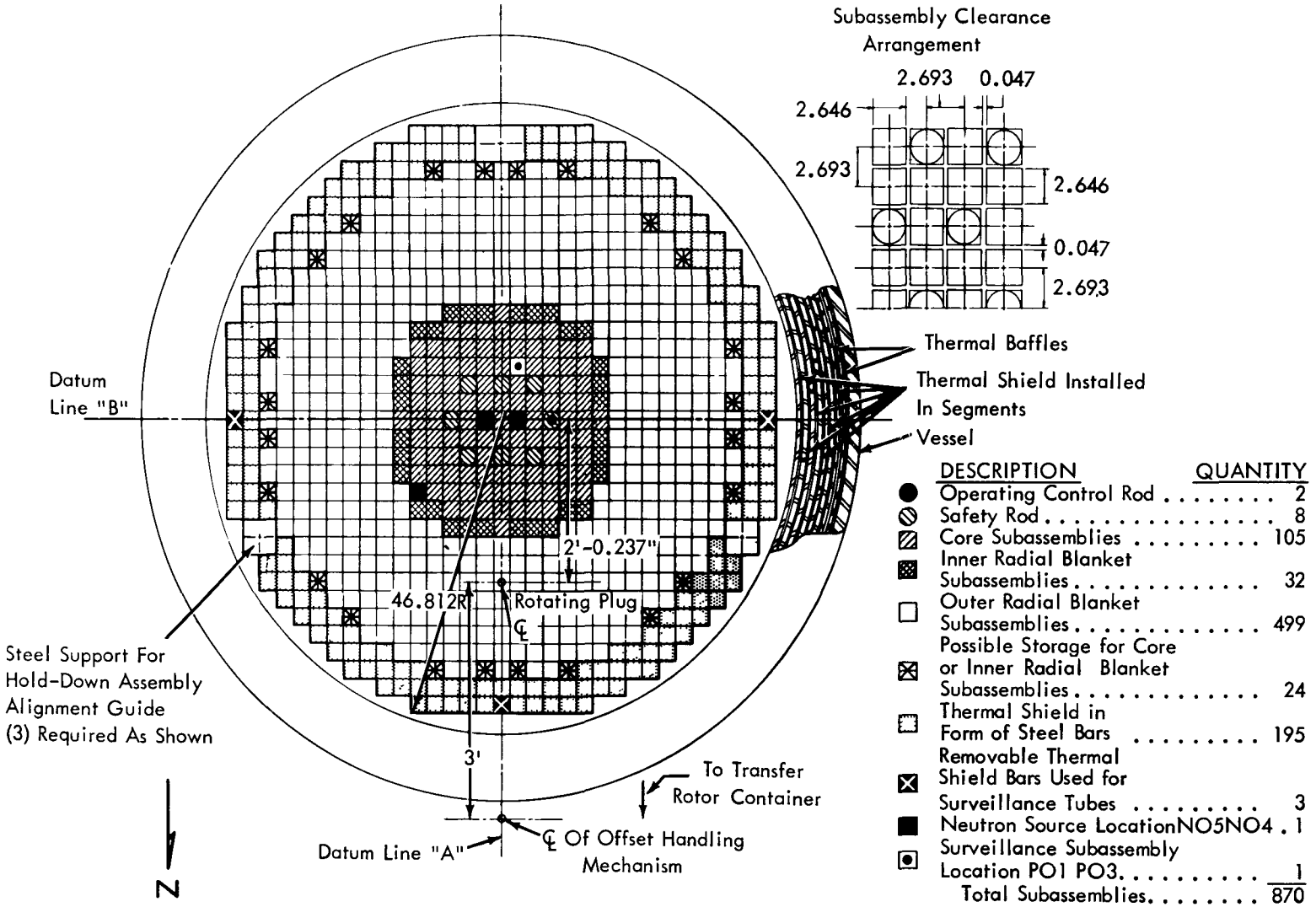


**FIG. 2 REACTOR CROSS SECTION**

The lattice positions surrounding the inner radial blanket contain the outer radial blanket subassemblies. Beyond the outer radial blanket are lattice positions used for stainless-steel-filled thermal shield bar subassemblies. These subassemblies provide thermal and neutron shielding for the reactor vessel. The outer radial blanket and shielding lattice positions are each supplied with sodium coolant from a low-pressure plenum.

The reactor is controlled by two operating control rods and seven safety rods, which are uniformly spaced around the center of the core. Provision for an eighth safety rod has been included in the design of the plant. The rods, all driven and actuated from the top, are of the poison type containing boron carbide ($B_4C$) in which the boron is enriched in boron-10 (B-10). One operating control rod is used for regulating purposes and the other for shimming. The average reactivity insertion rates of the two control rods are approximately one cent per second and one cent per minute, respectively. Each control rod has a reactivity worth of approximately 46 cents (~147 ih). The seven safety rods are worth more than $1.00 (~319 ih) each and provide shutdown reactivity. During operation of the reactor, the safety rods are held just above the upper axial blanket section of the core so that they can be rapidly inserted into the core if it becomes necessary to scram the reactor. During a normal shutdown, the safety rods are driven slowly into the core, where they remain during refueling to provide the necessary shutdown reactivity.

A more detailed description of the Fermi reactor may be found in the Enrico Fermi Hazards Summary Report.[1]

## B. POWER-REACTIVITY EFFECTS

### 1. General

The power coefficient of the reactor is defined as the reactivity change per unit of power change (¢/Mwt) at constant flow. It results from the fuel and coolant temperature changes which occur throughout the reactor when power is changed. These temperature changes are directly proportional to the power change but their magnitude differs, depending on location due to the temperature distribution in the reactor. The local temperature changes give rise to local Doppler and thermal expansion effects in the fuel, and local coolant and structural material expansion effects. These effects result in local reactivity changes. The local reactivity feedback effects intergrated over the entire reactor volume per unit of power change give the power coefficient.[1]

The power coefficient as defined above is constant at all powers, for constant flow, except for small perturbations resulting from nonlinearities in the program of reactor inlet temperature variation with power and

from small changes with temperature of the Doppler and material thermal expansion coefficients.

Flow changes affect the power coefficient in two ways: (1) those components of the power coefficient related to coolant temperature change vary inversely as flow and (2) those components related to fuel temperature change have one portion which varies inversely as flow and another portion which is independent of flow. These effects result from the fact that the coolant temperature rise across the core varies inversely as flow, whereas the temperature rise from cladding to fuel is independent of flow, i.e., it is only power-dependent. Because of this, the Doppler and fuel expansion components of the total power coefficient are somewhat less affected by flow changes than are the other coolant-temperature-related components.

The flow coefficient of the reactor may, therefore, be defined as the change in power coefficient with flow, i.e., the reactivity change per unit of flow change per thermal megawatt (¢/lb/hr/Mwt).

From the discussion above, it is apparent that the power coefficient and isothermal temperature coefficient are closely related: The power coefficient is essentially the temperature coefficient appropriately weighted by the local temperature changes per unit of power change throughout the reactor. For simplicity, discussion of power reactivity effects in the Fermi reactor is, therefore, given below in terms of temperature coefficients.

2. Temperature Coefficients

The Doppler coefficient is the only true nuclear temperature coefficient in the reactor. All other components of the total temperature coefficient result from changes in either the reactor compositon or reactor geometry due to thermal expansion of the core fuel, coolant, and steel structure, plus similar but lesser effects in the blanket. All of the compcompents are predicted to be negative, except a small positive subassembly bowing coefficient.

The Doppler coefficient is a small reactivity effect resulting from the broadening of the uranium fuel cross-section resonances with increased temperature. This results in more neutron captures in U-238, a negative reactivity effect, and more fissions in U-235, a positive effect. Theory indicates that the two opposing reactivity effects are approximately equal in magnitude for a U-238 to U-235 atomic ratio of one. In the Fermi reactor core, this atomic ratio is about three; consequently, the net Doppler effect is predicted to be negative.

The largest predicted temperature coefficient results from the radial core expansion which occurs as the reactor temperature increases. This expansion includes both the radial expansion of the steel subassembly

wrapper cans at their point of contact near the core midplane and the radial expansion of the upper and lower support structures of the core lattice. The reactivity effect of this expansion is negative, because it causes fuel to be shifted radially outward in the core to a position of lesser worth.

The sodium temperature coefficient is another large contributor to the total temperature coefficient in the reactor. As the sodium coolant in the core is heated, it expands and the sodium density is decreased. In the Fermi reactor, the sodium coolant has a positive reactivity worth because the principal effect of the sodium is to reduce neutron leakage from the reactor; therefore, the reactivity effect due to a decrease in sodium density when heated is of opposite sign, or negative.

The other major component of the temperature coefficient in the reactor is the reactivity effect resulting from expansion of the core fuel pins. As the fuel temperature increases, the fuel pins expand both axially and radially inside their subassembly wrapper cans. The axial fuel pin expansion moves fuel axially outward toward the core edge and the radial expansion of the fuel pins causes a displacement of sodium within the subassembly cans. The temperature coefficients resulting from these two thermal expansions are, therefore, analogous to those resulting from the core radial expansion and the core sodium expansion, respectively, and their values, although smaller, are also negative.

The other components of the temperature coefficient are small effects due to similar thermal expansions of the blanket fuel, blanket coolant, blanket structure, and holddown mechanism.

## C. PREDICTED TEMPERATURE AND POWER COEFFICIENTS

As described earlier, the components of the total temperature and power coefficients of reactivity in the Enrico Fermi reactor are the Doppler coefficient and various coefficients due to thermal expansion of the reactor fuel, coolant, and structure. The total coefficient is given by the sum of the individual components.

The predicted values for each component were based on calculations described in detail in Reference 1. These represent early calculations made before the reactor design was completely finalized; therefore, although based on critical experimental data, the values contain some known errors. The results of more recent calculations are given in Section V of this report but, for the present, only the early reference calculations will be considered.

The method of calculating the temperature and power coefficients was briefly the following: the Doppler coefficient was calculated by a statistical method[2] which included inelastic neutron scattering but assumed isolated resonances, i.e., the method used the narrow resonance approximation.

The integral effect over the entire core at 550 F was obtained by the method used. This was sufficient for the isothermal Doppler temperature coefficient predictions, where uniform temperature distribution throughout the reactor is assumed. For the power coefficient Doppler predictions, the value had to be corrected for local temperature variations, assuming the Doppler coefficient varies inversely as the three halves power of the absolute temperature.

The expansion temperature coefficients, resulting from slight movement of core materials to locations of different reactivity worth upon temperature increase, were calculated by perturbation theory. More specifically, the expansion reactivity effects were calculated as the sum of the effects resulting from local temperature variations throughout the reactor. To do this, local temperature coefficients for each component were first found which gave the reactivity effect of a unit change of local temperature or temperature gradient. These were obtained from structural deflection calculations using local material danger coefficients of reactivity found in the critical experiment.[3] Then, to obtain the isothermal temperature coefficients, local temperature coefficients were integrated numerically over the entire reactor volume. To obtain the power coefficients, local temperature coefficients were weighted by distribution of the derivative of temperature with respect to power within the reactor before integrating, since temperature response at power is position-dependent.

An important point in the definition of the Fermi power coefficient should be noted: The operating program for the reactor called for the coolant inlet temperature to be increased linearly with power from 517 to 550 F over the power range of 0 to 200 Mwt. However, for ease of calculation, the total reactivity override in going to power was separated into an isothermal override from 517 F to 550 F, obtained by integrating the isothermal temperature coefficient over this temperature range, and a power override in which the coolant inlet temperature is maintained constant at 550 F while the reactor power is raised from 0 to 200 Mwt. Although during actual reactor operation both the isothermal and power reactivity feedback occur simultaneously, all future mention of the power coefficient in this report refers only to the power override portion of the feedback which would occur if the inlet temperature were held constant. This is primarily done to be consistent with the definition used in the early calculations; however, such a division does have some physical significance also. For example, because inlet temperature changes with power are more or less arbitrarily controlled by the flows and other heat transfer parameters chosen for use in the secondary sodium and steam loops and effectively result in just a raising or lowering of the base temperature of the reactor, they tell nothing about the effect on reactivity of the power distribution in the reactor itself. A truer indication of the effect of the power distribution on reactivity is given by the power coefficient definition used above.

A summary of the original temperature and power coefficient predictions and override data based on 200 Mwt operation is given in Table I. The separation of the total feedback and override at power into an isother-

TABLE I - PREDICTED TEMPERATURE AND POWER COEFFICIENTS OF REACTIVITY

| Component | Isothermal Range | | Power Range | | | | |
|---|---|---|---|---|---|---|---|
| | Temperature Coefficient, $10^{-6}$ Δk/k/C | Override, ¢ | Temperature Coefficient, $10^{-6}$ Δk/k/C | Power Coefficient, ¢/Mwt | Override, ¢ | Base Temperature | Total Override, ¢ |
| Core | | | | | | | |
| Sodium Expansion | -4.44 | 1.22 | -4.16 | -0.0209 | 4.18 | Average Na | 5.40 |
| Fuel Pin Radial Expansion | -0.36 | 0.10 | 0.33 | -0.0030 | 0.61 | Average Fuel | 0.71 |
| Fuel Pin Axial Expansion | -5.80 | 1.61 | -6.96 | -0.0650 | 12.96 | Average Fuel | 14.57 |
| Doppler | -2.59 to -2.47 | 0.70 | -2.47 to -1.68 | -0.0189 (avg) | 3.78 | Fuel | 4.48 |
| Bowing | - | - | +0.44 | +0.0023 | -0.46 | Average Na | -0.46 |
| Lower Support Expansion | -1.47 | 0.43 | - | - | - | Inlet Na | 0.43 |
| Subassembly Wrapper Tube Radial Expansion | -11.33 | 3.14 | -17.96 | -0.0942 | 18.84 | Average Na | 21.98 |
| Holddown Plate Expansion | 0.02 | -.01 | 0.02 | +0.0002 | -0.04 | Exit Na | -0.05 |
| Inner Radial Blanket (IRB) | | | | | | | |
| Sodium Expansion | -1.70 | 0.47 | -1.70 | -0.0089 | 1.78 | IRB Na, Avg | 2.25 |
| Pin Expansion | -0.24 | 0.07 | -0.24 | -0.0022 | 0.45 | IRB Alloy, Avg | 0.52 |
| Displacement Due to Core Expansion | -0.67 | 0.17 | -0.63 | -0.0033 | 0.66 | Average Na | 0.83 |
| Displacement Due to Holddown Expansion | -0.28 | 0.08 | -0.14 | -0.0015 | 0.29 | Exit Na | 0.37 |
| Axial Blanket (AB) | | | | | | | |
| Sodium Expansion | -5.22 | 1.44 | -2.61 | -0.0274 | 5.48 | Exit Na | 6.92 |
| Axial Expansion | -0.09 | 0.02 | -0.04 | -0.0007 | 0.13 | UAB Alloy, Avg | 0.15 |
| Radial Expansion | -0.06 | 0.02 | -0.06 | -0.0002 | 0.06 | Average Na | 0.08 |
| Displacement Due to Holddown Expansion | -0.42 | 0.12 | -0.21 | -0.0020 | 0.44 | Exit Na | 0.56 |
| Totals | -34.56 | 9.58 | | -0.2458 | 49.16 | | 58.74 |

NOTE: The reactivity conversions for the Fermi reactor are

1 cent = 3.19 inhours (ih)
1 ih = $2.08 \times 10^{-5}$ Δk/k
$\beta_{eff}$ = 0.00662

mal and power component is clearly evident in the table. In particular, the absence of power coefficient components due to lower support plate and lower axial blanket expansions at the reactor inlet should be noted. The power coefficients given are based on full Core A flow ($2.95 \times 10^6$ lb/hr/loop, 3-loop operation). For the case of two-thirds Core A flow, the predicted total power coefficient is 1.41 times larger than the value of -0.246 ¢/Mwt given in the table, or -0.346 ¢/Mwt. The reason the total power coefficient does not vary exactly as inverse flow is the previously discussed flow-independent term in the components related to fuel temperature. Approximately 20% of the total power coefficient was predicted to be flow-independent.

Also given in Table I are at-power temperature coefficients defined with respect to various average temperatures, such as the average fuel temperature or average coolant temperature. These coefficients, which give the reactivity change for a one-degree change in average base temperature, were needed for reactor simulation work and were obtained by multiplying the power coefficients by the derivative of power with respect to the selected average temperature. They may also be derived from the isothermal temperature coefficient values by appropriately weighting them by the temperature distribution in the reactor with respect to the selected base temperature. Each component of the power coefficient, therefore, has a value given by the product of its at-power temperature coefficient times the derivative of its average base temperature with respect to power.

# III. EXPERIMENTAL PROCEDURE

## A. DESCRIPTION OF TEST

The four power coefficient measurements of the Enrico Fermi reactor were made in accordance with a detailed, preplanned procedure.[4] Prior to the conduct of the test, the procedure was reviewed for completeness and safety. Revisions were made to incorporate improvements, and additional steps were added where necessary to facilitate the acquisition of complete and precise data during the test. The procedure was also the basis used by the Fermi plant operating staff in preparation of operating guides for the conduct of the test.

The four measurements were made in essentially the same manner, by measuring the change in critical rod position as reactor power was increased or decreased, except that different maximum power levels and flows were used. The measurements coincided with the Fermi reactor high-power nuclear test program schedule. In this program, a six-step power and flow escalation schedule was followed in the approach to 100 Mwt from zero-power.[1,5] Basically, the six steps consisted of a series of physics measurements made during alternate reactor operation using nominal two- and three-loop flow at nominal power levels of 1.3, 2.0, 13.3, 20.0, 66.7, and 100 Mwt. However, no power coefficient measurements were made at the first two steps because of the lack of sensible heating at these low powers, and, consequently, meaningful feedback. The dates of each of the measurements and the nominal power levels (maximum) and flows used were as follows:*

---

* Besides the measurements listed, a number of unofficial power coefficient measurements were also made. These are described in detail in the Appendix A. For example, measurements were sometimes made during the approach to power for other tests. Also, 66.7 Mwt power coefficient data were obtained when this test was first attempted on June 23, 1966, but prematurely terminated by an unscheduled scram due to loss of flow in one of the two operating loops. None of these data are reported here because the measurements were not made as accurately as in the official tests.

TABLE II - POWER COEFFICIENT MEASUREMENTS

| Number | Date, 1966 | Nominal Power, Mwt | Nominal Flow, $2.95 \times 10^6$ lbs/hr/loop |
|---|---|---|---|
| 1 | January 13 | 13.3 | Two-Thirds (2 Loops) |
| 2 | February 1 | 20.0 | Full (3 Loops) |
| 3 | June 24 | 66.7 | Two-Thirds (2 Loops) |
| 4 | July 12 | 100.0 | Full (3 Loops) |

It should be emphasized that the power levels and flows given are nominal values. During the early testing at relatively low powers (67 Mwt or less), heat balance data were not yet available to accurately calibrate the power and flow recording instrumentation; such data were available during the later testing at higher powers. Therefore, for the early measurements the flow and power settings were based on preoperational and low-power test (<1 Mwt) instrument calibrations, whereas heat-balance calibration data were used in later measurements. This resulted in considerable variation from the nominal power and flow values in some of the tests.

As stated previously, all the power coefficient measurements were made in basically the same manner. The primary sodium flow was first adjusted to the desired value, and critical rod position reactivity measurements were then made at various power levels. A nominal power level of about 500 kwt was used as a base level; several powers in the middle of the power range were investigated; and measurements were made at the maximum designated test power. In each case, care was taken to ensure that the power stabilized before making the measurements. Also, the measurements were made during power descent as well as power ascent.

During each critical rod measurement the following data were obtained and logged: the time, critical rod position, reactor power level and power drift rate, primary sodium flow, reactor inlet and outlet temperatures, core inlet temperature, and core outlet temperatures at selected subassembly positions. The reactivity data obtained were then corrected for burnup effects, for changes in core inlet temperature, for any flow changes that might have occurred, and for power and flow instrumentation calibration errors when these data became known. Finally, the power coefficient was found by obtaining graphically the derivative of the curve of net reactivity as a function of power.

## B. REACTOR LOADING AND PLANT CONDITIONS

The core configuration, which was the same for each of the four power coefficient measurements, is shown in Figure 3.* This loading was used throughout the major portion of the high-power test program. It provided sufficient excess reactivity (approximately 89 cents at zero-power and a 517 F isothermal reactor start-up temperature) to accommodate the estimated override needed in going up to full 200 Mwt power and the anticipated burnup losses during testing.

As seen in Figure 3, the high-power oscillator rod was located in the reactor in place of safety rod No. 5 in core position P03-P00** throughout the test period. The oscillator rod was always set at its zero perturbation position (0 degree) during the power coefficient tests. This was done so that the data taken in the various tests would be directly comparable.

Normal reactor operating conditions were generally maintained during the tests; however, manual reactor control was used rather than automatic, since it allowed better control over the reactor test parameters. No abnormal interlock conditions were required for the measurements. As a safety measure, the reactor power level scram was adjusted to 130% of the maximum power of any given measurement.

The primary sodium system heat transport loops were operated at 100% flow per loop ($2.95 \times 10^6$ lbs/hr/loop)*** with two loops operating for measurements No. 1 and 3 and with three loops operating for measurements No. 2 and 4. Once the desired flow had been established, special effort was made to maintain a constant flow throughout the test, since flow changes

---

* A number of times during the course of the testing several core subassemblies were removed to storage positions during shutdown periods and later either returned to their original positions or replaced by other identical core subassemblies. However, these loading changes did not affect the basic core configuration shown in Figure 3.

** The coordinate system used to locate subassemblies in the core lattice is shown in Figure 3. The first position number given is the X coordinate and the second the Y coordinate. The letter P stands for positive values and the letter N for negative values; the core center is P00-P00.

*** The programmed total loop flow of $2.95 \times 10^6$ lb/hr consists of a flow of $2.56 \times 10^6$ lb/hr in the 14-inch line feeding the high pressure inlet plenum and $0.39 \times 10^6$ lb/hr in the 6-inch line to the low pressure inlet plenum.

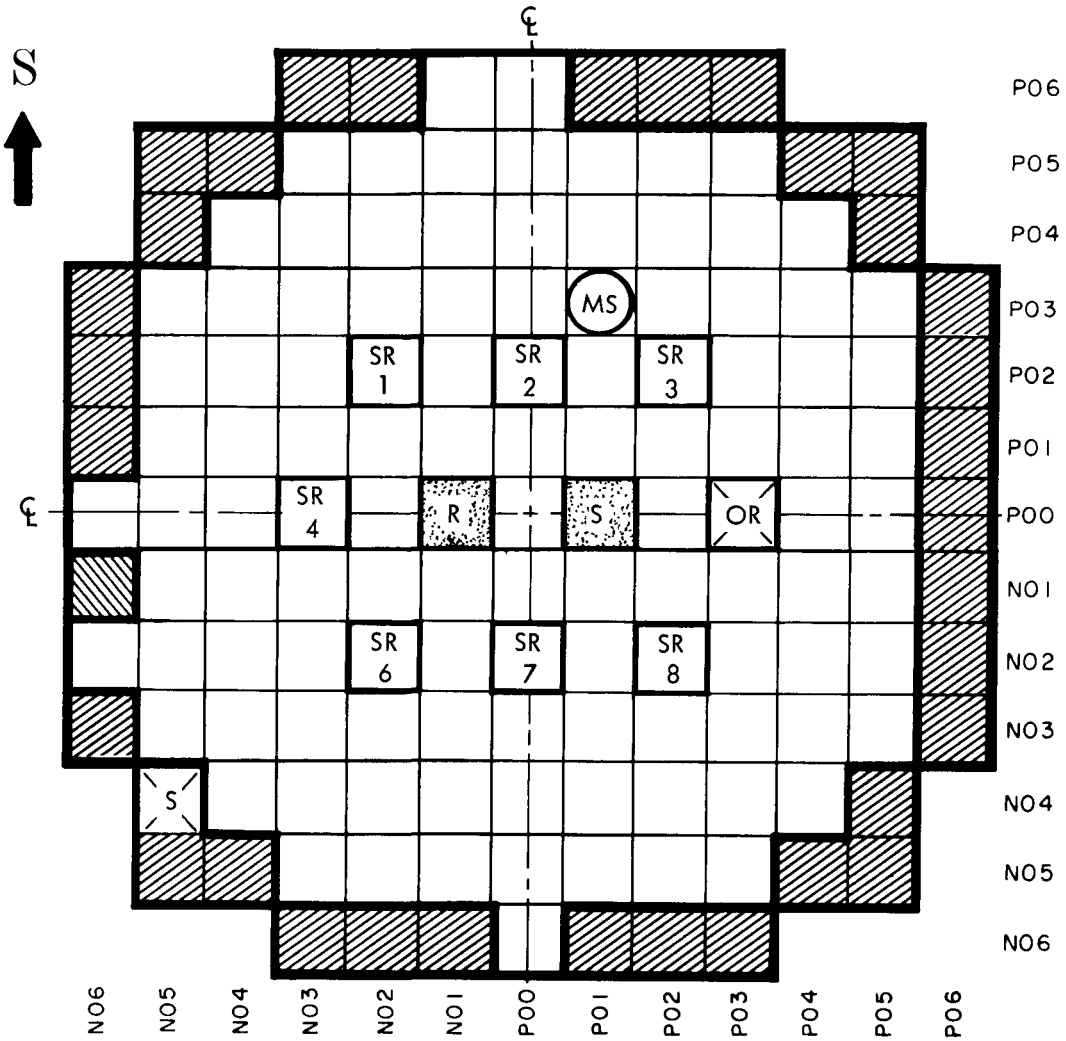


| DESCRIPTION | | QUANTITY |
|---|---|---|
| | Operating Control Rods ($B_4C$) | 2 |
| SR | Safety Rods ($B_4C$) | 7 |
| | Core Subassemblies (25.6 o/o enriched U-10 w/o Mo alloy; ~4.74 kg U-235 per subassembly) | 103 |
| MS | Materials Surveillance Subassembly (stainless steel, zirconium samples, etc.) | 1 |
| OR | Oscillator Rod ($B_4C$) | 1 |
| S | Neutron Source Subassembly (Sb-Be) | 1 |
| | Inner Radial Blanket Subassemblies (depleted U-3 w/o Mo alloy) | 34 |
| | | 149 |

**FIG. 3 CORE LOADING FOR POWER COEFFICIENT MEASUREMENTS**

would have markedly affected the feedback reactivity. The steam and feedwater system was operated according to established operating procedures to maintain the temperature of the sodium leaving the steam generators at 517 F. With the above conditions, the plant temperatures were always within their normal operating limits.

## C. INSTRUMENTATION

The parameters of interest in the test were the reactor power level, control rod positions, and primary sodium system temperatures and flows. Although heat balance data (secondary sodium, feedwater and steam system temperatures and flows) were taken simultaneously with the power coefficient data, they were not pertinent to the results of this test and are reported elsewhere.[6]

### 1. Nuclear Instrumentation

The permanent neutron detectors which provide signals to the plant's two source-range, three intermediate-range, and five power-range channels are located in six neutron-counter tubes (NCT) which penetrate the graphite shield surrounding the reactor vessel (Figure 1). Fission counters and ion chambers (uncompensated and compensated) are used for this purpose, and their placement in the various NCT's and original calibration are discussed in detail in References 7 and 8.

The original calibration of this instrumentation for absolute power was made by means of in-core absolute fission counter measurements. The measurements were made at low power ( < 1 Mwt) and the resulting calibration had an inherent inaccuracy of $\sim \pm 10\%$. Later on, various changes in the detector positions were made and, as a result, the over-all uncertainty in the original power calibration was increased to $\sim \pm 20\%$. At the time of the early power coefficient measurements these were the only calibration data available. Later recalibration of this instrumentation, using more accurate data obtained from heat balances, reduced the power calibration uncertainty to $\sim \pm 5\%$, as discussed in IV. C. 1.

The power indicated by these ten channels of nuclear instrumentation was read during the test from the recorder charts located on the main control console and logged. However, these data were not considered sufficiently accurate for use in the power coefficient analysis because of chart resolution limitations. Therefore, an additional power level measurement for this purpose was obtained using the signal from a spare ion chamber located in NCT-5 and connected to a Keithley micromicroammeter linear recorder located in the reactor control room. The Keithley channel was intercalibrated with the other instrumentation and by switching ranges on the micromicroammeter it could be used to accurately determine reactor

power from a few kilowatts up to full 100 Mwt power. The micromicroammeter was also used to determine the neutron flux (power) drift during the critical rod position reactivity measurements. From these data reactivity corrections for power drift could be made.

2. Rod Position Measurements

The critical positions of the two operating control rods during the test were determined from Gilmore digital indicators located on the control console which are connected to position potentiometers located on the rod drives. These have an estimated reading accuracy of $\pm$0.03-inch rod elevation. The rod position data were converted to reactivity data using the rod calibration curves.

3. Temperature Sensing Instrumentation

Eleven measurements of primary system temperature were made in the test, using five thermocouples and six resistance temperature detectors, all of which are part of the normal plant instrumentation. Each of the thermocouples was connected through a switch to a common potentiometer and the resistance temperature detectors were similarly connected to a common resistance bridge. With this high-accuracy readout instrumentation, which was calibrated in a preoperational test, temperatures could be read to an estimated accuracy of $\pm$1 F.

Four of the five thermocouples which were read are mounted in the fingers of the holddown mechanism and monitor the core sodium temperatures at the outlet of three core subassemblies and one inner radial blanket subassembly. The fifth thermocouple, located on the core lower support plate (Figure 1), monitors the sodium temperature at the core inlet.

The six resistance temperature detectors which were read are located in the piping of the primary sodium system. There is one in each of the three 30-inch sodium pipes that leave the reactor and one in each of the three 6-inch inlet pipes that supply the low-pressure (blanket) inlet plenum to the reactor (Figure 1). These detectors monitor the reactor outlet and inlet temperatures, respectively.

To analyze the test results, only the inlet temperature data were actually required. These data were needed to make the reactivity corrections to account for inlet temperature changes with power and obtain power coefficient values consistent with the definition used for the Fermi plant (see II. C).

The outlet temperature data were only used as an aid in determining that the reactor had stablized at the desired test power level before making reactivity measurements. To ensure stabilization, the requirement

was set that all primary system temperatures should be within ±2 F of their previous readings and the power drift less than 5%, over a 5-minute interval.

The observed temperature rise across the core ($T_{out}$-$T_{in}$) was also used as an indication that the reactor power-to-flow ratio was properly set during the test.

4. Flow Measurements

Six measurements of primary system sodium flow were made in the test, using the electromagnetic flowmeters which are part of the normal plant instrumentation. Two flowmeters are installed in each of the three primary loops. One is located in the 14-inch line of each loop which feeds the core and inner radial blanket high-pressure plenum and one is located in the 6-inch line of each loop which feeds the outer radial blanket low-pressure plenum. The voltage signals from the flowmeters are monitored by calibrated flow recorders located in the reactor control room and the flows were read there. The total flow in each loop was given by the sum of the 14-inch and 6-inch flows. The uncertainty in the initial preoperational calibration of these instruments was estimated to be approximately ±10%. Later recalibration of these instruments from heat balance data reduced the uncertainty to ~ ±5%, as discussed in Section IV. C. 1.

The flow data were used to ensure that the proper flow existed prior to the test and to ensure that no significant flow changes occurred during the test.

# IV. EXPERIMENTAL DATA AND DATA ANALYSES

The experimental data obtained in the power coefficient measurements consisted of power, flow, temperature, and critical rod position data. The final heat balance correction factors for power and flow were not obtained until all measurements were completed. For this reason, the data are first reported as originally recorded, i.e., based on the initial power and flow calibrations. The results of the subsequent initial data analyses are then given. Finally, the corrected data analyses are given. This procedure is followed so that the chronological history of the measurements is maintained. As will be seen later, this procedure is significant in understanding some of the conclusions reached from the tests.

## A. EXPERIMENTAL DATA

The data initially obtained in the four measurements are summarized in Tables III and IV. In all cases the reactor was at equilibrium (III. C. 3) before the measurements were made. This can be seen from the fact that the power drift was either zero or very small in all the measurements; it is also illustrated by the fact the temperature changes between measurements made at the same power level were negligible (for example, see Table IV, Fourth Measurement, Data Points 7 and 8). As indicated, the power and flow data are based on the initial power and flowmeter calibrations. Only the Keithley micromicroammeter power is given for the reason mentioned earlier (III. C. 1). The flows are given for both the 14-inch and 6-inch lines in each loop. The total flow through the reactor in each loop is the sum of these values. As can be seen, the total flow per loop in the measurements was sometimes substantially different than the programmed test flow of $2.95 \times 10^6$ lb/hr/loop, as explained in III. A. It may also be noted that when only two loops were in operation, backflow occurred in the shutdown loop. When determining total flow, this had to be subtracted from the total flow for the other two loops.

Since the oscillator rod was always at its 0-degree position during the measurements, only the critical control rod positions are given. As seen, the shim rod was kept fully inserted (0-inch elevation) during all measurements, and only the faster-moving regulating rod was used to make power adjustments.

A study of the temperature information in the tables shows that the temperatures and temperature changes at the various sensor locations during the measurements were generally consistent with anticipated behavior. However, some peculiar temperature behavior can be seen; this behavior

TABLE III - DATA FROM THE FIRST AND SECOND POWER COEFFICIENT MEASUREMENTS

| Nominal Conditions | Date | Data Point No. | Time, hr | Keithley Power, Mwt | Power Drift Rate, % per 5 minutes | Critical Rod Positions, Inches Withdrawn | | Primary Sodium Flowmeter Flows, $10^6$ lb/hr | | | | | | Reactor Inlet Temp., F | | | Core Inlet Temp. at Lower Support Plate, F | Core and Inner Radial Blanket Outlet Temp., F | | | | Reactor Outlet Temp., F | | | Miscellaneous Data |
|---|---|---|---|---|---|---|---|---|---|---|---|---|---|---|---|---|---|---|---|---|---|---|---|---|---|
| | | | | | | | | Loop 1 | | Loop 2 | | Loop 3 | | | | | | | | | | | | | |
| | | | | | | Reg. Rod | Shim Rod | 14 in. | 6 in. | 14 in. | 6 in. | 14 in. | 6 in. | Loop 1 | Loop 2 | Loop 3 | | Core 1 | Core 2 | Core 3 | IRB | Loop 1 | Loop 2 | Loop 3 | |
| **FIRST MEASUREMENT** | | | | | | | | | | | | | | | | | | | | | | | | | |
| 13.3 Mwt Maximum Power<br>Two-Loop (2/3 flow) Operation | January 13, 1966 | 1 | 0905 | 0.492 | 0 | 3.40 | 0 | 2.75 | 0.285 | -0.45 | 0.24 | 2.45 | 0.285 | 518.30 | 520.20 | 529.45 | 518.62 | 519.75 | 519.20 | 519.42 | 518.75 | 522.35 | 518.25 | 519.40 | |
| | | 2 | 1018 | 6.80 | 0 | 3.52 | 0 | 2.75 | 0.285 | -0.45 | 0.24 | 2.55 | 0.285 | 513.75 | 513.95 | 526.40 | 513.00 | 533.10 | 526.25 | 528.95 | 520.0 | 528.00 | 523.40 | 528.85 | The integrated power during the measurement was ~2.8 Mwd. |
| | | 3 | 1112 | 13.13 | 0 | 4.02 | 0 | 2.75 | 0.29 | -0.45 | 0.245 | 2.50 | 0.285 | 514.50 | 513.35 | 521.20 | 511.50 | 551.25 | 538.40 | 543.60 | 526.50 | 539.35 | 528.00 | 532.20 | |
| | | 4 | 1211 | 13.13 | 0 | 3.96 | 0 | 2.75 | 0.285 | -0.45 | 0.245 | 2.50 | 0.285 | 514.60 | 514.55 | 521.05 | 512.70 | 553.40 | 540.35 | 545.65 | 528.15 | 540.00 | 532.50 | 535.00 | |
| | | 5 | 1435 | 13.11 | 0 | 3.92 | 0 | 2.75 | 0.285 | -0.45 | 0.245 | 2.50 | 0.285 | 513.75 | 511.40 | 519.70 | 511.65 | 552.20 | 538.85 | 544.45 | 526.95 | 537.35 | 530.15 | 532.05 | |
| | | 6 | 1550 | 6.45 | 0 | 3.59 | 0 | 2.80 | 0.285 | -0.45 | 0.245 | 2.55 | 0.285 | 514.90 | 518.55 | 525.20 | 514.35 | 533.70 | 527.15 | 529.85 | 521.20 | 529.50 | 523.95 | 524.00 | |
| | | 7 | 1700 | 0.483 | 0 | 3.11 | 0 | 2.75 | 0.285 | -0.45 | 0.245 | 2.45 | 0.285 | 514.75 | 514.85 | 524.85 | 514.50 | 516.05 | 515.30 | 515.70 | 514.85 | 519.90 | 515.10 | 515.00 | |
| **SECOND MEASUREMENT** | | | | | | | | | | | | | | | | | | | | | | | | | |
| 20.0 Mwt Maximum Power<br>Three-Loop (full flow) Operation | February 1, 1966 | 1 | 1135 | 0.489 | 0 | 4.20 | 0 | 2.60 | 0.40 | 2.55 | 0.41 | 2.55 | 0.40 | 516.0 | 516.4 | 527.9 | 516.00 | 520.6 | 519.5 | 519.6 | 516.0 | 522.8 | 517.2 | 518.9 | |
| | | 2 | 1330 | 10.15 | 0 | 4.82 | 0 | 2.60 | 0.40 | 2.55 | 0.41 | 2.55 | 0.40 | - | - | - | 516.10 | 535.9 | 529.9 | 533.4 | 523.4 | 531.2 | 525.5 | 527.9 | |
| | | 3 | 1435 | 19.85 | 0 | 5.48 | 0 | 2.60 | 0.40 | 2.60 | 0.41 | 2.55 | 0.40 | 521.6 | 518.1 | 531.7 | 516.40 | 556.5 | 544.1 | 551.9 | 531.7 | 545.0 | 535.5 | 540.8 | |
| | | 4 | 1545 | 9.85 | 0 | 4.90 | 0 | 2.60 | 0.41 | 2.60 | 0.41 | 2.55 | 0.40 | 518.2 | 517.1 | 531.0 | 516.70 | 536.3 | 534.3 | 530.3 | 524.0 | 531.7 | 527.5 | 528.8 | |
| | | 5 | 1715 | 0.487 | 0 | 4.28 | 0 | 2.60 | 0.41 | 2.60 | 0.41 | 2.50 | 0.40 | 516.6 | 517.0 | 528.4 | 516.80 | 517.0 | 516.9 | 517.3 | 516.5 | 521.2 | 518.3 | 517.3 | The integrated power during the measurement was ~2.35 Mwd. |

TABLE IV - DATA FROM THE THIRD AND FOURTH POWER COEFFICIENT MEASUREMENTS

| Nominal Conditions | Date | Data Point No | Time, hr | Keithley Power, Mwt | Power Drift Rate, % per 5 minutes | Critical Rod Positions, Inches Withdrawn | | Primary Sodium Flowmeter Flows, $10^6$ lb/hr | | | | | | Reactor Inlet Temp., F | | | Core Inlet Temp. at Lower Support Plate, F | Core and Inner Radial Blanket Outlet Temp., F | | | | Reactor Outlet Temp., F | | | Miscellaneous Data |
|---|---|---|---|---|---|---|---|---|---|---|---|---|---|---|---|---|---|---|---|---|---|---|---|---|---|
| | | | | | | Reg Rod | Shim Rod | Loop 1 | | Loop 2 | | Loop 3 | | | | | | | | | | | | | |
| | | | | | | | | 14 in | 6 in | 14 in | 6 in | 14 in | 6 in | Loop 1 | Loop 2 | Loop 3 | | Core 1 | Core 2 | Core 3 | IRB | Loop 1 | Loop 2 | Loop 3 | |
| THIRD MEASUREMENT | | | | | | | | | | | | | | | | | | | | | | | | | |
| 66.7 Mwt Maximum Power<br>Two-Loop (2/3 flow) Operation | June 24, 1966 | 1 | 0825 | 0.496 | 0 | 3.93 | 0 | 2.5 | 0.25 | 2.50 | 0.23 | -0.4 | 0 24 | 512.7 | 514.0 | 512.4 | 518.4 | 514.8 | 514.8 | 514.8 | 514.0 | 513.8 | 514.6 | 513.0 | The integrated power during the measurement was ~15.0 Mwd. |
| | | 2 | 1040 | 39.40 | 0 | 8.69 | 0 | 2.60 | 0.25 | 2.58 | 0.23 | -0.4 | 0.24 | 528.9 | 529.8 | 528.8 | 533.5 | 663.4 | 618.3 | 652.5 | 578.5 | 602.0 | 586.2 | 595.5 | |
| | | 3 | 1328 | 65.70 | 0 | 12.79 | 0 | 2.58 | 0.26 | 2.60 | 0.23 | -0.4 | 0.24 | 541.6 | 541.8 | 541.3 | 546.5 | 735.0 | 697.0 | 749.2 | 626.0 | 667.8 | 668.8 | 661.0 | |
| | | 4 | 1539 | 40.0 | 0 | 8.96 | 0 | 2.5 | 0.25 | 2.60 | 0 23 | -0.4 | 0.24 | 530.5 | 531.9 | 532.0 | 534.8 | 670.6 | 625.0 | 658.0 | 583.2 | 608.0 | 620.0 | 606.2 | |
| | | 5 | 1711 | 13.27 | 0 | 6.36 | 0 | 2.5 | 0.25 | 2.60 | 0.23 | -0.4 | 0.24 | 528.4 | 527.2 | 527.4 | 531.6 | 573.5 | 558.2 | 570.2 | 543.7 | 552.6 | 559.1 | 550.4 | |
| | | 6 | 1842 | 0.970 | 0 | 4.08 | 0 | 2.5 | 0.24 | 2.60 | 0.23 | -0 4 | 0.23 | 512.5 | 513.5 | 512.5 | 516.6 | - | 514.14 | 515.2 | 512.9 | 513.0 | 514.2 | 515.4 | |
| FOURTH MEASUREMENT | | | | | | | | | | | | | | | | | | | | | | | | | |
| 100 Mwt Maximum Power<br>Three-Loop (full flow) Operation | July 12, 1966 | 1 | 0835 | 0.249 | 0 | 5.41 | 0 | 2.7 | 0.42 | 2.70 | 0.42 | 2.8 | 0.42 | 519.6 | 520.1 | 520.3 | 525.1 | 520.6 | 520.4 | 520.6 | 520.0 | 519.8 | 520.9 | 520.4 | The integrated power during the measurement was ~37.14 Mwd. |
| | | 2 | 1015 | 19.98 | -1.5 | 6.74 | 0 | 2.7 | 0.42 | 2.75 | 0.42 | 2.85 | 0.42 | 522.3 | 524.6 | 526.2 | 529.4 | 562.5 | 549.8 | 559.4 | 537.7 | 545.5 | 542.1 | 546.3 | |
| | | 3 | 1055 | 40.30 | -0.4 | 8.25 | 0 | 2.7 | 0.42 | 2.70 | 0.42 | 2.90 | 0.42 | 528.2 | 531.1 | 533.3 | 534.5 | 606.9 | 580.7 | 600.4 | 556.8 | 572.5 | 561.6 | 572.8 | |
| | | 4 | 1148 | 59.40 | 0 | 9.88 | 0 | 2.7 | 0.42 | 2.75 | 0.40 | 3.00 | 0.40 | 531.4 | 537.4 | 540.3 | 541.0 | 652.0 | 612.5 | 640.5 | 576.9 | 601.1 | 593.7 | 602.3 | |
| | | 5 | 1330 | 80.40 | 0 | 11.67 | 0 | 2.7 | 0.42 | 2.80 | 0.42 | 2.90 | 0.42 | 536.4 | 541.3 | 544.4 | 545.6 | 694.3 | 642.1 | 680.6 | 595.4 | 627.6 | 622.6 | 626.3 | |
| | | 6 | 1515 | 99.35 | 0 | 13.76 | 0 | 2.7 | 0.42 | 2.80 | 0.42 | 2.82 | 0.43 | 540.5 | 546.0 | 550.1 | 545.6 | 735.1 | 669.6 | 717.5 | 612.8 | 651.9 | 646.5 | 651.2 | |
| | | 7 | 1615 | 109.40 | 0 | 15.57 | 0 | 2.7 | 0.42 | 2.80 | 0.42 | 2.95 | 0.43 | 544.2 | 548.8 | 554.2 | 548.0 | 756.3 | 684.0 | 738.5 | 622.0 | 666.8 | 659.6 | 665.2 | |
| | | 8 | 1725 | 109.40 | 0 | 15.32 | 0 | 2.75 | 0.42 | 2.75 | 0.42 | 3.00 | 0.43 | 542.1 | 547.0 | 552.8 | 545.8 | 756.3 | 684.2 | 738.8 | 621.2 | 665.8 | 662.0 | 664.8 | |
| | | 9 | 1800 | 99.35 | 0 | 13.66 | 0 | 2.75 | 0.42 | 2.75 | 0.42 | 2.80 | 0.42 | 537.8 | 542.1 | 545.8 | 542.0 | 737.2 | 669.2 | 719.0 | 611.3 | 651.7 | 651.3 | 651.0 | |
| | | 10 | 1855 | 79.20 | 0 | 11.41 | 0 | 2.75 | 0.42 | 2.75 | 0.42 | 2.76 | 0.42 | 534.4 | 537.4 | 541.7 | 537.4 | 691.6 | 638.5 | 677.4 | 592.2 | 624.5 | 625.6 | 624.0 | |
| | | 11 | 1950 | 59.70 | 0 | 9.81 | 0 | 2.72 | 0.42 | 2.70 | 0.41 | 2.65 | 0.42 | 530.2 | 533.1 | 535.9 | 532.6 | 650.6 | 610.1 | 640.3 | 574.4 | 598.9 | 599.1 | 600.1 | |
| | | 12 | 2020 | 40.0 | 0 | 8.28 | 0 | 2.70 | 0.41 | 2.65 | 0 41 | 2.50 | 0.41 | 525.6 | 527.3 | 529.9 | 526.9 | 607.6 | 579.8 | 601.2 | 555.2 | 572.9 | 574.6 | 572.9 | |
| | | 13 | 2055 | 19 69 | 0 | 7.17 | 0 | 2.70 | 0.41 | 2.65 | 0.41 | 2 70 | 0.41 | 525.8 | 524.8 | 525.1 | 527.7 | 568.1 | 554.3 | 564.4 | 541.5 | 549.0 | 548.7 | 549.0 | |
| | | 14 | 2137 | 0.770 | 0 | 5.64 | 0 | 2.70 | 0.40 | 2.60 | 0.40 | 2.53 | 0.41 | 519.1 | 518.8 | 519.4 | 518.0 | 519.6 | 518.8 | 519.5 | 518.1 | 518.1 | 522.8 | 518.9 | |

will be discussed later (see IV.B.1.e and IV.B.2). No indication is given of the core lattice positions at which the subassembly outlet temperatures were monitored, since this information was not important to the test results.

The last column in each table gives integrated power information which can be related to burnup reactivity effects.

## B. INITIAL DATA ANALYSES

The initial analyses of the data in Tables III and IV were made within a day or two after completion of each measurement. Because the original power and flowmeter calibrations were used, no concern was given to the fact that in some cases the metered flow during the test did not correspond exactly to the programmed test flow. It was realized that flow corrections would have to be made later when accurate flowmeter calibrations became available.

### 1. Method

The data from each measurement were analyzed as follows: First, the reactor excess reactivity corresponding to each data point (power level) was determined from the critical rod position data, and the values were corrected for any power drift, flow change, inlet temperature change, or burnup reactivity perturbations which occurred during the measurements. The corrected reactivity values were then normalized to the first (zero power) reactivity measurement and plotted against power. Next, a least-squares curve fit was made to the data, the slope of which gave the desired power coefficient value. A more detailed explanation of the method used is given below.

#### a. Critical Rod Reactivities

The reactor excess reactivity was found from the critical rod position data using the regulating rod calibration curve shown in Figure 4.[9] Since the shim rod remained fully inserted throughout the test, the calibration curve for it was not needed; only the fully-shadowed regulating rod curve shown in Figure 4 was used.

In practice, the difference in critical rod position between the first (zero power) data point and the data point of concern was determined. The excess reactivity loss at the power of the data point of concern relative to the first data point was then found by multiplying this difference by the slope of the rod calibration curve over the position range in question (see Figure 4). In this way, the critical reactivities were automatically normalized to the first measurement. Also, greater accuracy was obtained for the case of small rod position changes than could have been obtained by

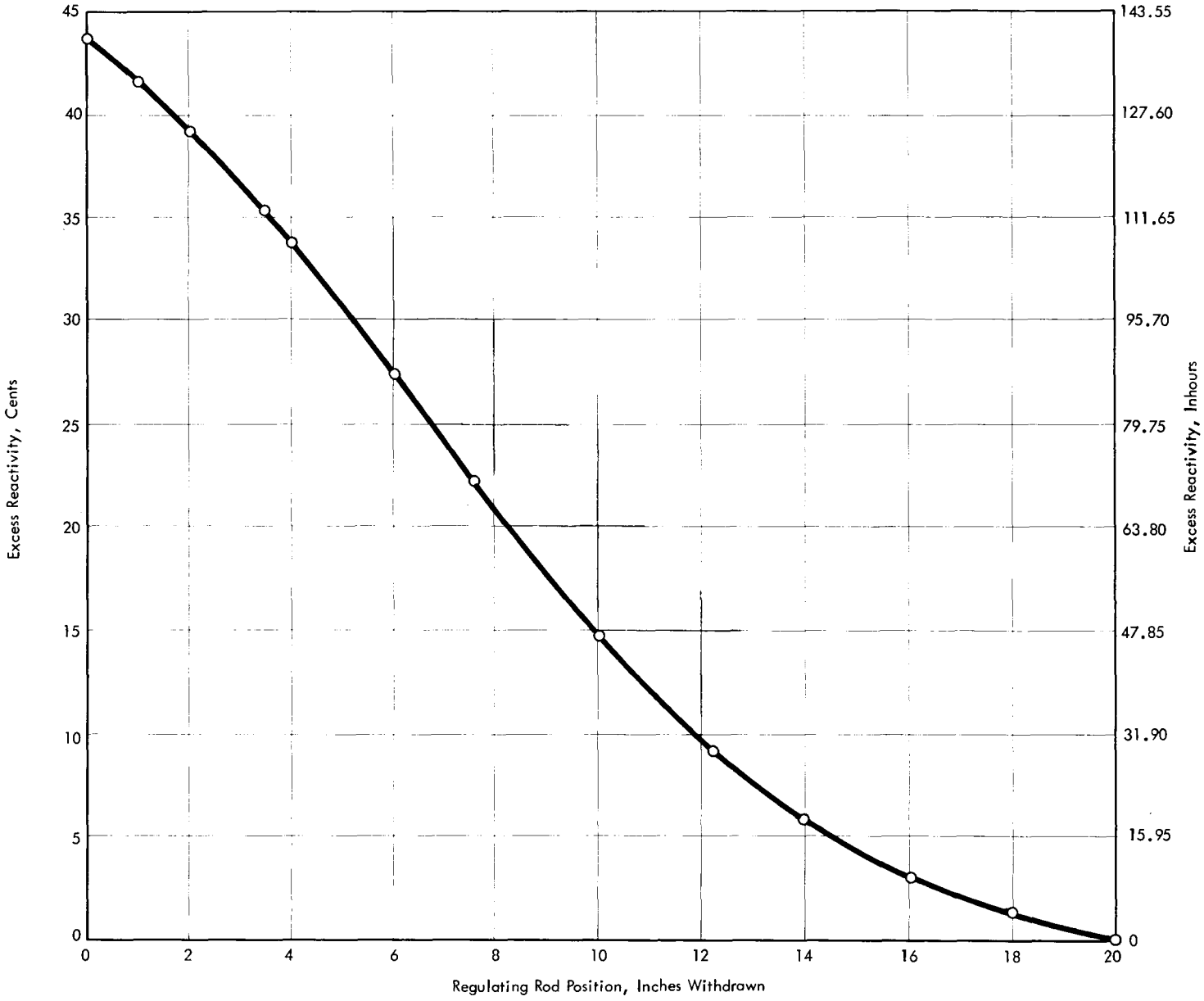


**FIG. 4 EXCESS REACTIVITY VERSUS CRITICAL REGULATING ROD POSITION (FULLY SHADOWED)**

taking readings directly from the calibration curve. Of course, when the rod position change was large, the slope was not constant over the full range, and direct readings had to be used.

b. Power Drift Correction

Power drift corrections were made to the critical rod reactivity data if the reactor was not exactly critical at the time of the reactivity measurement. Only two data points required such corrections, i.e., Data Points No. 2 and 3 of the Fourth Measurement (Table IV). These were made using the calculated correction factor, $\Delta\rho = 0.12$ ih per one per cent drift in five minutes.[10] Upward (positive) drift was a negative correction and vice versa.

c. Effect of Flow Changes

Reactor flow strongly affects power-reactivity feedback; consequently, it was important during the measurements to ensure that the flow remain very nearly constant. Otherwise reactivity corrections would have had to be made to account for flow changes. From Tables III and IV, it can be seen that flow changes during the measurements were insignificant. The largest variation, approximately $\pm 3\%$, occurred during the 100 Mwt 3-loop measurements. This variation was assumed to be negligible and within the flowmeter reading error. Therefore, no flow corrections were made in the initial analyses.

d. Burnup Corrections

To accurately compare all reactivity data in a measurement to the first (zero-power) data point, the effect of burnup reactivity losses during the test period had to be taken into account. Although this was not important and no corrections were made for the two low-power measurements made at 13 Mwt and 20 Mwt, it was important for the 67 Mwt and 100 Mwt measurements. The data points were corrected for burnup by determining the integrated power (Mwd) during the run corresponding to each point and multiplying this value by the calculated burnup loss rate of -0.051 ih/Mwd.[11] This loss rate assumes no Pu-239 production in the reactor during a run and was used because the runs were short compared to the half-life of Np-239, the plutonium's precursor. The burnup reactivity loss calculated for each data point was subtracted from the critical rod reactivity loss to correct for burnup.

e. Inlet Temperature Corrections

The critical rod reactivity data also had to be corrected for inlet temperature variations between data points. This was required because the power coefficient is defined for constant inlet temperature. The correc-

tions for all data points of a measurement were made relative to the inlet temperature of the first (zero power) data point. To make the correction, the differences in inlet temperature between the first data point and all other data points were determined and multiplied by -0.82 ih/F, the isothermal temperature coefficient value measured during the low-power tests.[12] For data points having higher inlet temperatures than the first point, the reactivity correction was negative (subtracted from the critical rod reactivity loss); for lower temperatures, the reactivity correction was positive. The choice of inlet temperature readings used in making the corrections varied between measurements, however, as explained below.

At the time of the first two power coefficient measurements, the inlet temperature readings obtained appeared peculiar (see Table III). The reactor inlet and core inlet temperatures did not increase with power as expected, and the reactor inlet temperatures were appreciably different for each of the three loops. Also, the average of the reactor inlet temperatures was not equal to the core inlet temperature, as would be expected if the reactor inlet temperatures were actually different and uniform mixing in the lower plenum occurred.* It was noticed too that the core inlet temperature did not return to its initial value following power ascent and power descent; instead it returned to a lower value. However, little concern was given to this point at the time, since the over-all temperature behavior was so erratic.

The reasons for these peculiarities were not fully understood at the time; thus, it was somewhat arbitrarily decided that the core inlet temperature readings would be used for the initial 13 Mwt and 20 Mwt analyses. This decision was based mainly on the favorable experience exhibited by this temperature detector during the low-power test program, when its operation was found to be extremely reliable.

By the time the 67 Mwt and 100 Mwt power coefficient measurements were made, the reason for the reactor inlet temperature anomalies described above had been discovered and corrected. These anomalies occurred primarily because poor data on steam generator secondary sodium outlet temperatures were being obtained due to nonuniform mixing at the temperature sensor locations. In the Fermi reactor, the feedwater flow is controlled by these data, and the error in them was sufficient to produce the erratic reactor inlet temperature behavior that was seen. New steam generator sodium outlet temperature sensors were installed in each loop at locations further downstream than previously, and this problem was corrected by the time the 67 Mwt and 100 Mwt measurements were made (see Table IV).

---

* The 14-inch and 6-inch inlet lines in a loop both receive the same primary pump discharge sodium. It can, therefore, be assumed that the 6- and 14-inch line temperatures in each loop are identical.

With this problem solved, the 67 Mwt and 100 Mwt power coefficient data were analyzed by using inlet temperature corrections made with both the core inlet reading and the average of the three reactor inlet readings. However, as will be seen later (IV.B.2), there was still a significant difference in the power coefficient results, depending on which inlet temperature value was used.

f. Curve Fitting

The critical rod reactivities for each data point, corrected for power drift, burnup, and inlet temperature variations, gave the net reactivity loss. The data were plotted versus Keithley power for both the power ascent and the power descent modes of operation and a least-squares linear curve fit to the data was made. Actually, an exact linear variation is not really anticipated because of the material expansion coefficients and Doppler coefficient variations with temperature; however, these effects were expected to be small and an inspection of the experimental data revealed no obvious nonlinearities. Therefore, a linear fit was used.

2. Results

The results of the initial data analyses made by the above method are summarized in Tables V and VI. The critical rod excess reactivity losses for each data point are given, together with the various corrections made to obtain the net reactivity losses as a function of power. The net losses are plotted against power in Figures 5 through 10. The figures also show the least-squares linear fit to the data and the resulting slopes, i.e., the power coefficient values (¢/Mwt).

Figures 5 and 6, which show the results of the 13.3 Mwt 2-loop and 20 Mwt 3-loop measurements, respectively, required no drift, flow, or burnup corrections.* The only correction required was one to account for inlet temperature changes. As explained earlier, this was made using only the core inlet temperature readings in both cases. Figure 5 shows an apparent hysteresis effect when the power ascent curve is compared with the power descent curves, i.e., the power coefficient value measured during power as-

* The 2 to 3 Mwd integrated powers accumulated during each run amount to only 0.10 ih (0.03¢) to 0.15 ih (0.05¢) burnup reactivity corrections, and were neglected.

TABLE V - DATA ANALYSES - FIRST AND SECOND MEASUREMENTS

| Operating Conditions | Data Point No. | Keithley Power, Mwt* | Change in Critical Rod Position Relative to Data Pt. No. 1, Inches* | Loss in Excess Reactivity Relative to Data Pt. No. 1, ih | Change in Core Inlet Temperature Relative to Data Pt. No. 1, F* | Inlet Temperature Reactivity Correction, ih | Power Drift Reactivity Correction | Burnup Reactivity Correction | Net Excess Reactivity Loss Relative to First Data Point | |
|---|---|---|---|---|---|---|---|---|---|---|
| | | | | | | | | | Inhours | Cents |
| | | | | FIRST MEASUREMENT | | | | | | |
| 13.3 Mwt Maximum Power Two-Loop Operation Total Metered Flow=5.63 x $10^6$ lb/hr* | 1 | 0.492 | 0 | 0 | 0 | 0 | NONE | NEGLIGIBLE | 0 | 0 |
| | 2 | 6.80 | 0.12 | 1.20 | -5.62 | 4.62 | | | 5.82 | 1.82 |
| | 3 | 13.13 | 0.62 | 6.20 | -7.12 | 5.84 | | | 12.04 | 3.78 |
| | 4 | 13.13 | 0.56 | 5.60 | -5.92 | 4.84 | | | 10.44 | 3.28 |
| | 5 | 13.11 | 0.52 | 5.20 | -6.97 | 5.72 | | | 10.92 | 3.42 |
| | 6 | 6.45 | 0.19 | 1.90 | -4.27 | 3.50 | | | 5.40 | 1.69 |
| | 7 | 0.483 | -0.29 | -2.90 | -4.12 | 3.37 | | | 0.47 | 0.15 |
| | | | | SECOND MEASUREMENT | | | | | | |
| 20.0 Mwt Maximum Power Three-Loop Operation Total Metered Flow=8.95 x $10^6$ lb/hr* | 1 | 0.489 | 0 | 0 | 0 | 0 | NONE | NEGLIGIBLE | 0 | 0 |
| | 2 | 10.15 | 0.62 | 6.20 | 0.10 | -0.08 | | | 6.12 | 1.92 |
| | 3 | 19.85 | 1.28 | 12.80 | 0.40 | -0.33 | | | 12.47 | 3.91 |
| | 4 | 9.85 | 0.70 | 7.00 | 0.70 | -0.57 | | | 6.43 | 2.02 |
| | 5 | 0.487 | 0.08 | 0.80 | 0.80 | -0.65 | | | 0.15 | 0.05 |

* See Table III

TABLE VI - DATA ANALYSES - THIRD AND FOURTH MEASUREMENTS

| Operating Conditions | Data Point No. | Keithley Power, Mwt* | Change in Critical Rod Position Relative to Data Pt. No. 1, Inches* | Loss in Excess Reactivity Relative to Data Pt. No. 1, ih | Inlet Temperature Change Relative to Data Pt. No. 1, F* | | Inlet Temperature Reactivity Correction, ih | | Power Drift Reactivity Correction, Inhours | Integrated Power Relative to Data Pt. No. 1, Mwd | Burnup Reactivity Correction, Inhours | Net Excess Reactivity Loss Relative to First Data Point | | | |
|---|---|---|---|---|---|---|---|---|---|---|---|---|---|---|---|
| | | | | | | | | | | | | Core Inlet Temperature Corrected | | Reactor Inlet Temperature Corrected | |
| | | | | | Core | Reactor | Core | Reactor | | | | Inhours | Cents | Inhours | Cents |
| **THIRD MEASUREMENT** | | | | | | | | | | | | | | | |
| 66.7 Mwt Maximum Power Two-Loop Operation Total Metered Flow=5.42 x $10^6$ lb/hr* | 1 | 0.496 | 0 | 0 | 0 | 0 | 0 | 0 | NONE | 0 | 0 | 0 | 0 | 0 | 0 |
| | 2 | 39.40 | 4.76 | 48.8 | 15.1 | 16.2 | -12.4 | -13.3 | | 2.21 | -0.11 | 36.24 | 11.36 | 35.28 | 11.06 |
| | 3 | 65.70 | 8.86 | 82.3 | 28.1 | 28.6 | -23.0 | -23.4 | | 8.74 | -0.45 | 58.73 | 18.41 | 58.41 | 18.31 |
| | 4 | 40.0 | 5.03 | 51.4 | 16.4 | 18.5 | -13.4 | -15.2 | | 13.16 | -0.67 | 37.29 | 11.69 | 35.54 | 11.14 |
| | 5 | 13.27 | 2.43 | 24.3 | 13.2 | 14.7 | -10.8 | -12.1 | | 14.66 | -0.75 | 12.76 | 4.00 | 11.52 | 3.61 |
| | 6 | 0.970 | 0.15 | 1.5 | -1.8 | -0.2 | +1.5 | +0.16 | | 14.98 | -0.76 | 2.23 | 0.70 | 0.93 | 0.29 |
| **FOURTH MEASUREMENT** | | | | | | | | | | | | | | | |
| 100 Mwt Maximum Power Three-Loop Operation Total Metered Flow=9.61 x $10^6$ lb/hr | 1 | 0.249 | 0 | 0 | 0 | 0 | 0 | 0 | - | 0 | 0 | 0 | 0 | 0 | 0 |
| | 2 | 19.98 | 1.33 | 13.80 | 4.3 | 4.4 | -3.52 | -3.61 | 0.18 | 0.69 | -0.04 | 10.42 | 3.28 | 10.33 | 3.24 |
| | 3 | 40.30 | 2.84 | 29.50 | 9.4 | 10.9 | -7.71 | -8.94 | 0.05 | 1.52 | -0.08 | 21.76 | 6.82 | 20.53 | 6.43 |
| | 4 | 59.40 | 4.47 | 44.80 | 15.9 | 16.4 | -13.04 | -13.44 | - | 3.36 | -0.17 | 31.59 | 9.92 | 31.19 | 9.78 |
| | 5 | 80.40 | 6.26 | 59.60 | 20.5 | 20.7 | -16.80 | -17.0 | - | 9.61 | -0.50 | 42.30 | 13.25 | 42.10 | 13.20 |
| | 6 | 99.35 | 8.35 | 73.00 | 20.5 | 25.5 | -16.80 | -20.90 | - | 16.18 | -0.83 | 55.37 | 17.30 | 51.27 | 16.08 |
| | 7 | 109.40 | 10.16 | 81.80 | 22.9 | 29.1 | -18.80 | -23.80 | - | 20.55 | -1.05 | 61.95 | 19.40 | 56.95 | 17.82 |
| | 8 | 109.40 | 9.91 | 80.70 | 20.7 | 27.3 | -16.98 | -22.40 | - | 25.87 | -1.32 | 62.40 | 19.55 | 56.98 | 17.85 |
| | 9 | 99.35 | 8.25 | 72.70 | 16.9 | 21.9 | -13.88 | -17.98 | - | 28.42 | -1.45 | 57.37 | 17.97 | 53.27 | 16.69 |
| | 10 | 79.20 | 6.00 | 57.50 | 12.3 | 17.8 | -10.10 | -14.60 | - | 32.16 | -1.64 | 45.76 | 14.35 | 41.26 | 12.93 |
| | 11 | 59.70 | 4.40 | 44.30 | 7.5 | 13.1 | -6.15 | -10.72 | - | 35.08 | -1.79 | 36.36 | 11.39 | 31.79 | 9.97 |
| | 12 | 40.0 | 2.87 | 29.60 | 1.8 | 7.6 | -1.48 | -6.24 | - | 36.12 | -1.84 | 26.28 | 8.25 | 21.52 | 6.74 |
| | 13 | 19.69 | 1.76 | 18.10 | 2.6 | 5.2 | -2.13 | -4.26 | - | 36.85 | -1.88 | 14.09 | 4.22 | 11.96 | 3.75 |
| | 14 | 0.770 | 0.23 | 2.30 | -7.1 | -0.9 | +5.82 | +0.74 | - | 37.14 | -1.89 | 6.23 | 1.95 | 1.15 | 0.36 |

* See Table IV.

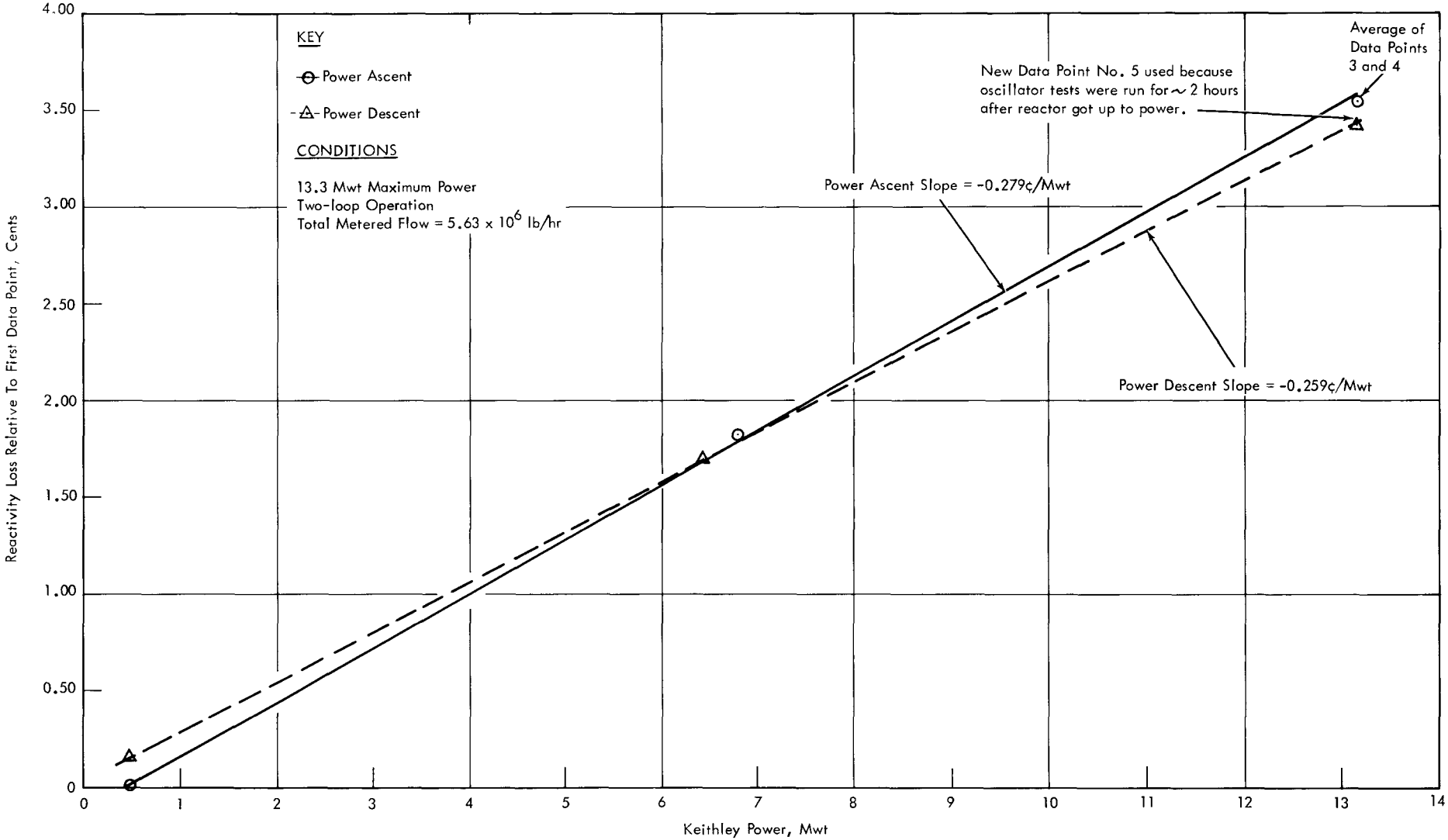


**FIG. 5 POWER COEFFICIENT MEASUREMENT NO. 1 CORRECTED FOR CORE INLET TEMPERATURE**

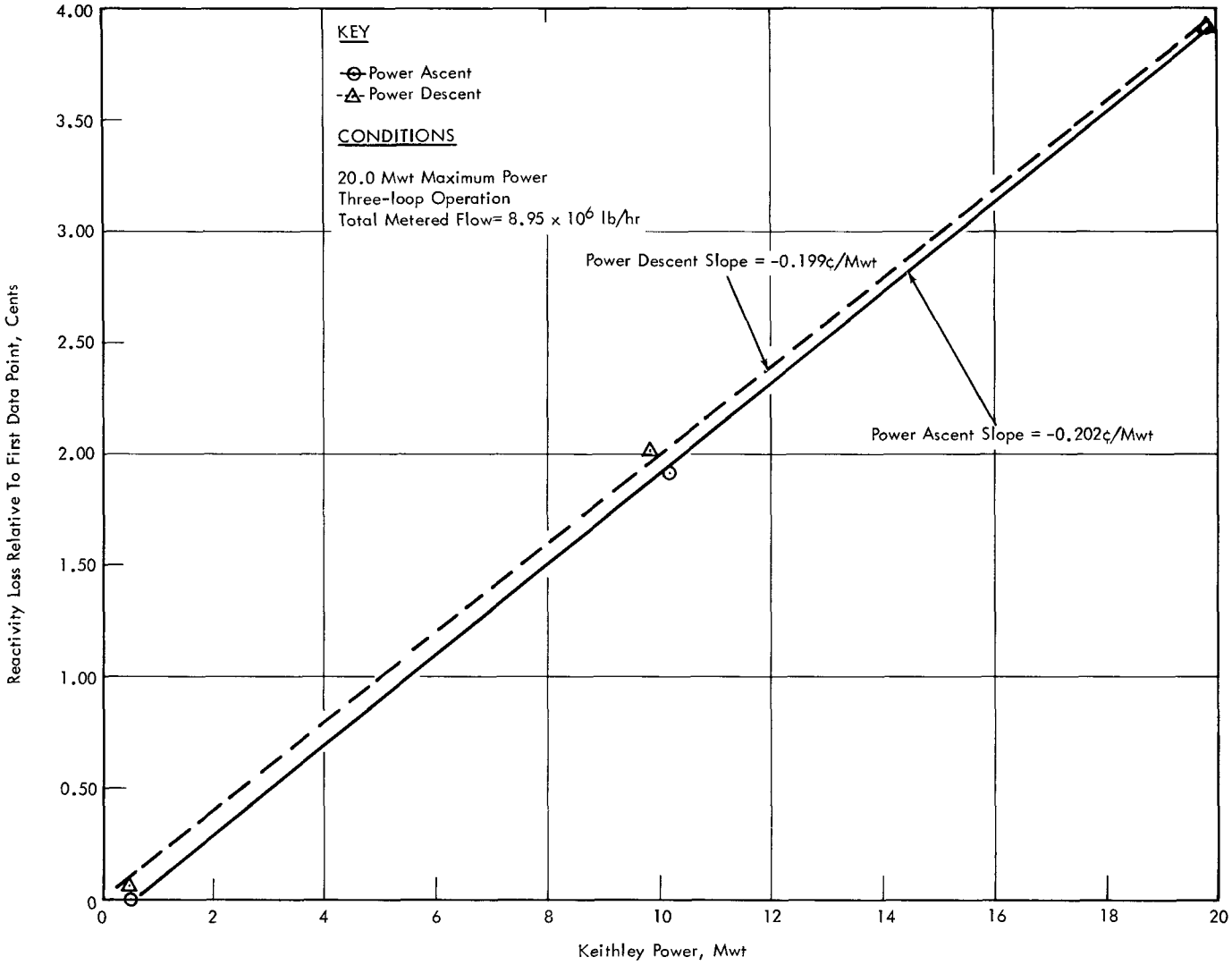


**FIG. 6 POWER COEFFICIENT MEASUREMENT NO. 2 CORRECTED FOR CORE INLET TEMPERATURE**



Figure 15a this side only

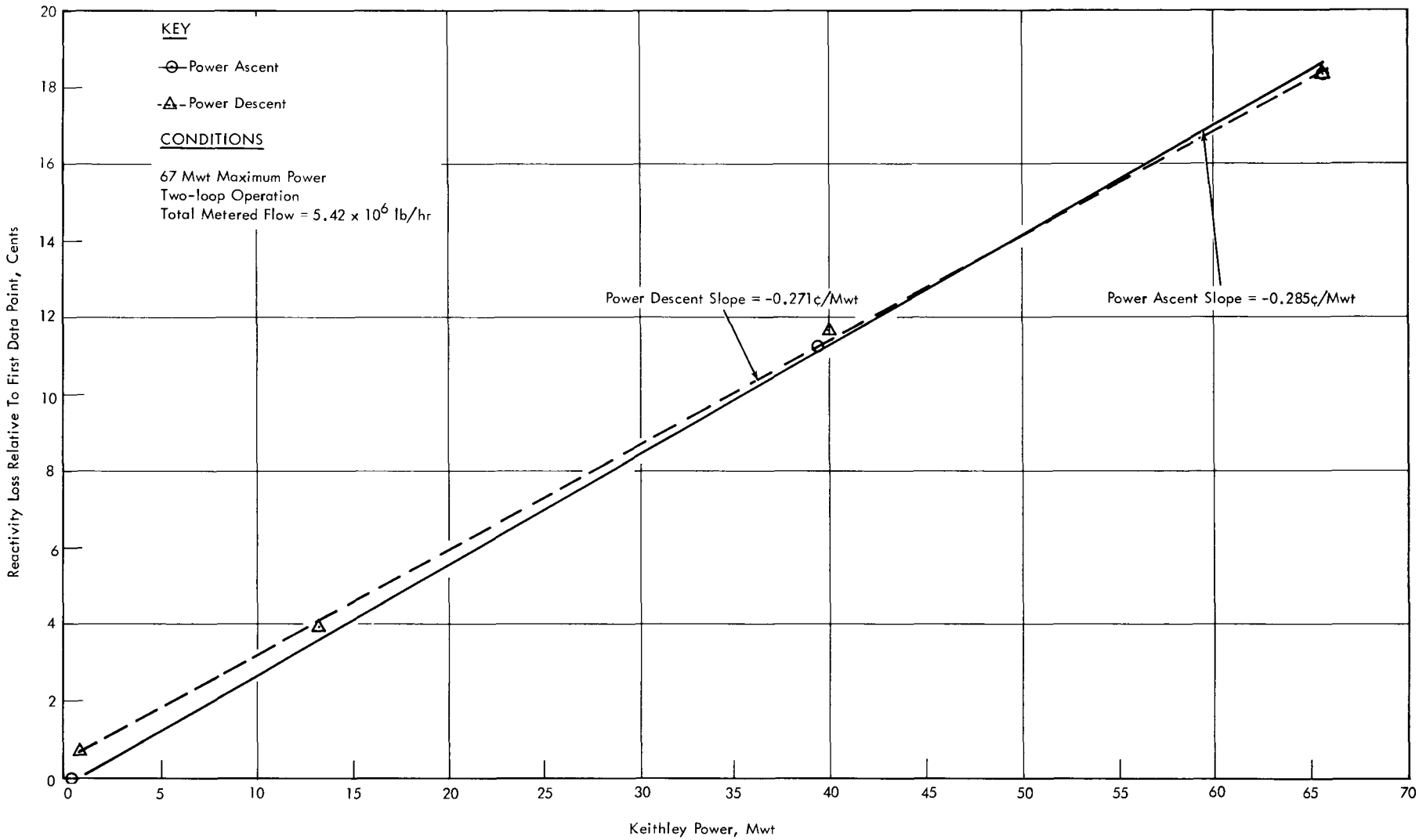


**FIG. 7 POWER COEFFICIENT MEASUREMENT NO. 3 CORRECTED FOR CORE INLET TEMPERATURE**

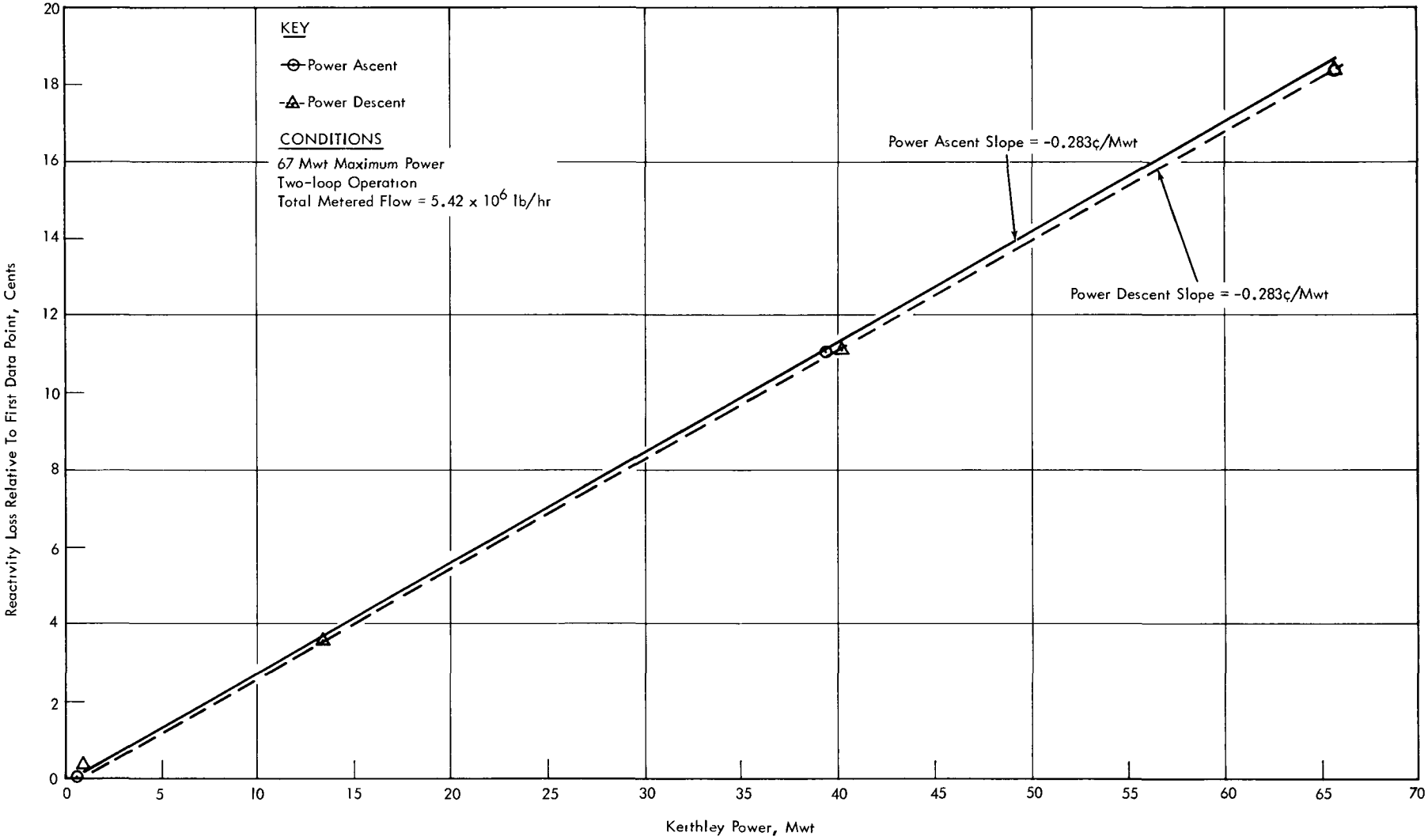


**FIG. 8 POWER COEFFICIENT MEASUREMENT NO. 3 CORRECTED FOR REACTOR INLET TEMPERATURE**

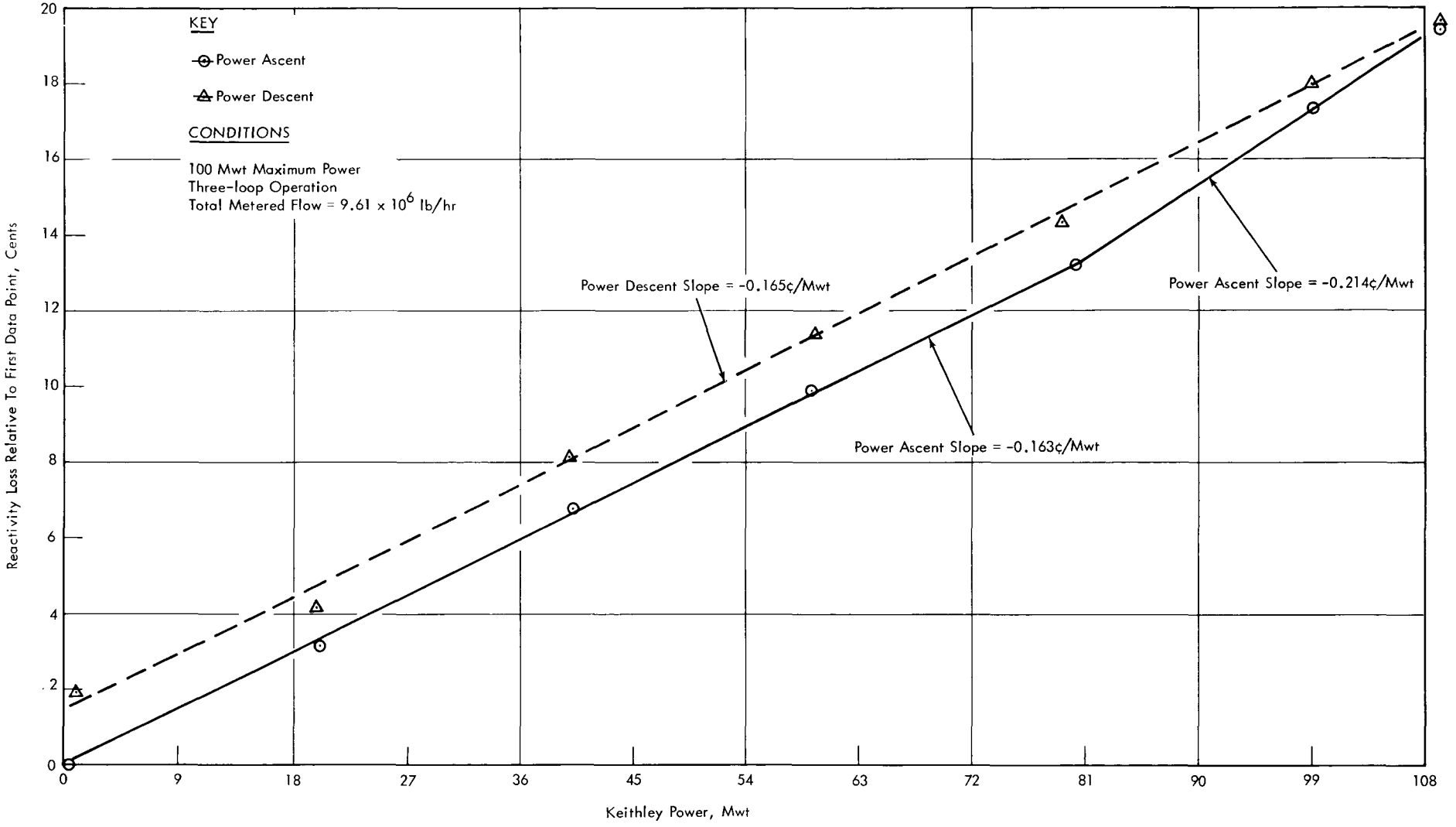


**FIG. 9 POWER COEFFICIENT MEASUREMENT NO. 4 CORRECTED FOR CORE INLET TEMPERATURE**

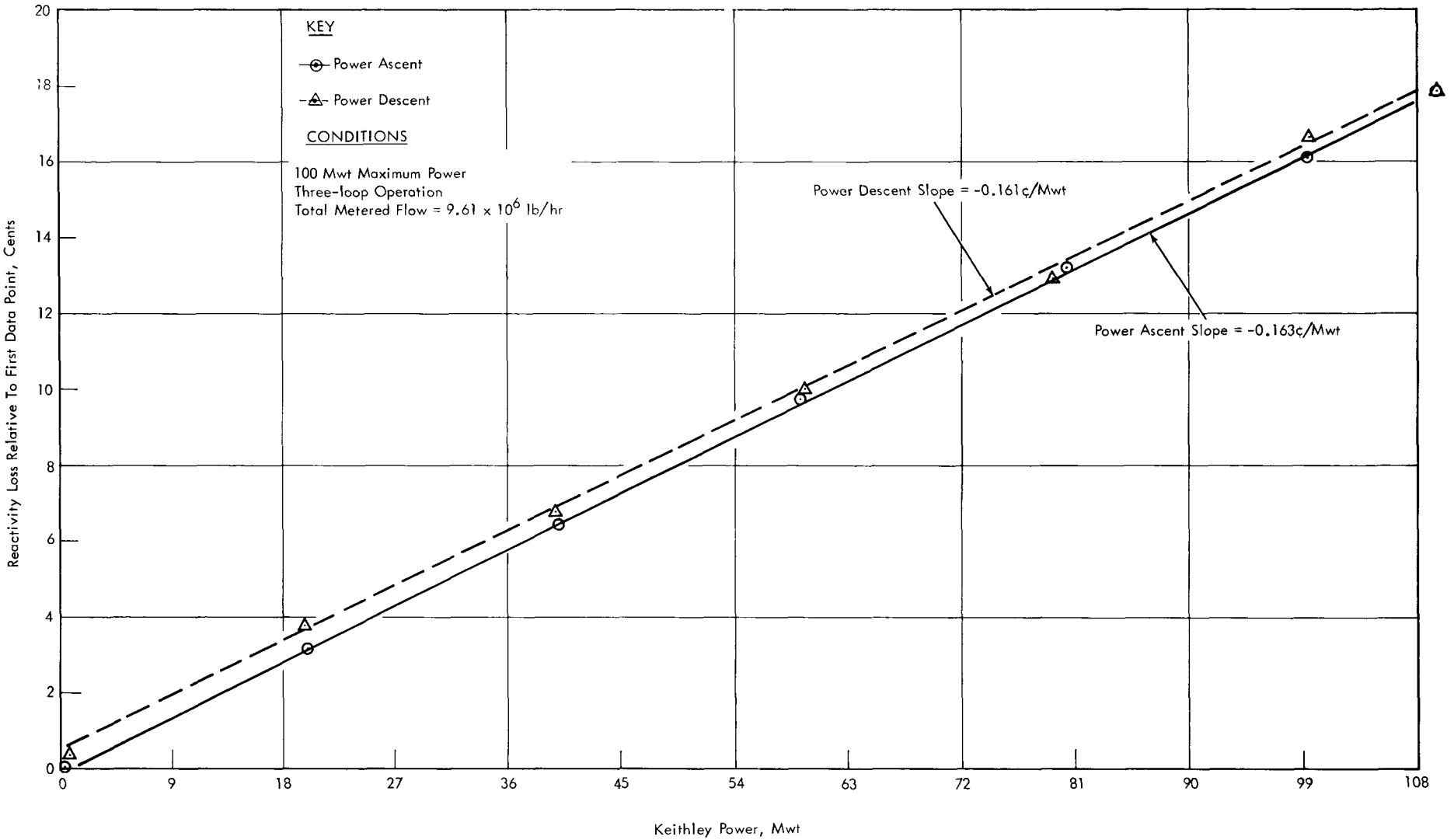


**FIG. 10 POWER COEFFICIENT MEASUREMENT NO. 4 CORRECTED FOR REACTOR INLET TEMPERATURE**

cent is larger than that measured during power descent, resulting in a net reactivity loss over and above burnup effects for the cycle.* This is similar to the behavior observed at EBR-II.[13] Figure 6 does not indicate any such effect, however.

Figures 7 through 10, which show the results of the 67 Mwt 2-loop and 100 Mwt 3-loop measurements, respectively, required drift and burnup corrections as well as inlet temperature corrections. Also, the inlet temperature corrections were made using both the core inlet (Figures 7 and 9) and reactor inlet (Figures 8 and 10) readings. As can be seen, the plots using core inlet temperature data show an apparent strong hysteresis effect while the others do not.

Because of the experience at EBR-II, it was first believed that the hysteresis behavior seen in the early power coefficient measurements was real. However, in view of the different results obtained later using both core and reactor inlet temperature data corrections, doubts were raised and further investigations made. The observed hysteresis behavior was eventually traced to the malfunctioning of a signal cable running from the junction box connection of the core inlet temperature thermocouple to the temperature readout station located in the main control room. The cable has since been replaced. The basic difficulty caused by this malfunction, which resulted in the apparent hysteresis, can be seen in Tables III and IV; namely, it was the fact that the core inlet temperature readings on power descent were generally smaller than those measured during power ascent at corresponding power levels. An extreme example of this is seen in Data Points No. 5, 6, 9 and 10 of the Fourth Measurement in Table IV. This behavior resulted in an inlet temperature reactivity correction that was too small for the power descent data points and, consequently, an apparent excess reactivity loss that was too large relative to the first data point, thereby producing the observed hysteresis.

From the above studies, it was decided that the most accurate analyses for the 67 Mwt and 100 Mwt measurements were those using reactor inlet temperature corrections (Figures 8 and 10). In the case of the 13 Mwt and 20 Mwt measurements (Figures 5 and 6), where only core inlet temperature data were used for the reasons explained earlier, it was decided that an

---

* If the small neglected burnup correction of $\sim 0.14$ ih is considered, the hysteresis effect becomes slightly smaller, i.e., the power ascent curve would become slightly flattened (a smaller power coefficient value) and the power descent curve would become slightly steepened (a larger power coefficient value). However, the effect of this correction on the hysteresis, as shown in Figure 5, is small.

average of the power ascent and power descent power coefficient values should be taken. On this basis, the power coefficient values from the initial analyses thought to be most accurate are those given below:

TABLE VII - INITIAL POWER COEFFICIENT VALUES

| Measurement No. | Operating Conditions | Total Loop Flow (14-in. plus 6-in. Lines) from Flowmeter Readings, $10^6$ lb/hr | Measured Power Coefficient, c/Mwt | Estimated Uncertainty |
|---|---|---|---|---|
| 1 | 13 Mwt 2-loops | 5.63 | -0.269 | $\pm$ 25% |
| 2 | 20 Mwt 3-loops | 8.95 | -0.200 | $\pm$ 25% |
| 3 | 67 Mwt 2-loops | 5.42 | -0.283 | $\pm$ 23% |
| 4 | 100 Mwt 3-loops | 9.61 | -0.162 | $\pm$ 23% |

The estimated uncertainty of approximately $\pm$ 25% given for these measurements is discussed below.

3. Error Analysis

The accuracy of the initial power coefficient measurement was determined primarily by the uncertainties in the reactor power and flow measurements. An additional but relatively small source of error was the reactivity measurement uncertainty. Certain assumptions had to be made regarding these uncertainties, however, since generally they had not been determined experimentally. Upper limits for each were, therefore, used in the error analyses and the power coefficient uncertainties found are probably conservative because of this.

Detailed error analyses for the initial power coefficient measurements, given in References 14 and 15,will not be repeated here; however, briefly they were made as follows:

a. The uncertainties in the reactivity and power measurements were determined and uncertainty flags obtained for each of the data points in Figures 5 through 10.

b. The reactivity and power uncertainties of each data point were combined to obtain the uncertainty in the power coefficient measured under test flow conditions.

c. The flow uncertainty was considered and combined with the power coefficient uncertainty for test flow conditions to obtain the total uncertainty in the experimentally determined power coefficient.

The reactivity measurement uncertainty was found using the following estimated (maximum) uncertainties in its five basic components: (1) critical regulating rod position determination ($\pm$ 0.03 inch, $\sim$ $\pm$ 0.30 ih), (2) rod calibration curve slope ($\pm$ 0.2 ih/inch), (3) inlet temperature determination ($\pm$ 1F, $\sim$ $\pm$ 0.82 ih), (4) isothermal temperature coefficient value ($\pm$ 0.02 ih/F), and (5) combination flux drift, burnup, and flow nonreproducibility uncertainty ($\pm$ 0.50 ih).

The most probable reactivity measurement error was taken to be the root mean square of the above five components. The rod position and inlet temperature measurement uncertainties each had to be included twice, however, since the data points in the plots were all referred to the initial zero power measurements. When this was done, a maximum reactivity measurement uncertainty of approximately $\pm$ 0.45¢ ($\pm$ 1.4 ih) was found for the reactivity data in the plots, amounting to about 22% of the average measured net reactivity loss in Table V and 5% of that in Table VI. The greater relative accuracy of the later measurements is due to the greater power range over which the measurements were made. This tends to reduce the relative effect of the reactivity uncertainty, although the absolute uncertainty for each data point is still the same for all measurements.

The accuracy of the reactor power level measurements using the Keithley micromicroammeter calibration was estimated to be $\pm$ 20% (III. C. 1). The same uncertainty applies also to the difference in measured power level between any two data points. This is true because of the way in which the power calibration was obtained, i.e., by directly scaling low-power data. Thus, the relative magnitude and sign of any power discrepancy existing due to calibration errors must be the same at all power levels.*

The most probable errors in the power coefficient values measured under test flow conditions were found by taking the root mean square of the power and reactivity uncertainties listed above. In doing this, allowance

---

* The small random uncertainty in the power measurements due to readout errors, ion chamber nonlinearity effects, etc., was neglected, since it was found to be negligible when compared to the calibration uncertainty.

was made for the fact that the effective reactivity uncertainties in the least-squares power coefficient determinations were only approximately one-half those quoted above for individual data points, i.e., 11% and 2-1/2%, respectively.* On this basis, the power coefficient uncertainties for test flow conditions were found to be ± 23% for the 13 Mwt and 20 Mwt measurements and ± 20% for the 67 Mwt and 100 Mwt measurements.

The last uncertainty in the measurements was the flow uncertainty which accounted for possible discrepancies between test flow conditions and the programmed two-loop and three-loop flows. The flow uncertainty was assumed to be ± 10% (III. C. 1) for all measurements and was taken to include the effects of both the variation in test flow between data points and flowmeter calibration errors. The corresponding uncertainty in the power coefficient measurements due to the flow uncertainty was therefore ± 10% also, using the simplfying assumption that the power coefficient varies inversely as flow.

The total uncertainty in the experimentally determined power coefficient was then found in each case by taking the root mean square of the uncertainty due to reactivity and power measurement errors and the uncertainty due to flow. On this basis, the total uncertainty in the power coefficient for programmed flow conditions was found to be ± 25% for the first two measurements and ± 23% for the last two measurements.

These can be regarded as maximum errors. As seen, they are primarily determined by power and flow uncertainties.

4. Preliminary Conclusions

From the initial analyses a number of preliminary conclusions were reached. However, the large uncertainty in the initial power coefficient values resulting from the power and flow uncertainties was an unknown factor that could not be easily taken into account in these early evaluations. As a result, several of the early conclusions are later shown to be not entirely valid (IV. C. 4); the preliminary conclusions may be summarized as follows:

a. The power coefficient values obtained in the first three measurements made at 13 Mwt 2-loop operation (-0.269 ¢/Mwt), 20 Mwt 3-loop operation (-0.200 ¢/Mwt), and 67 Mwt 2-loop operation (-0.283 ¢/Mwt) are consistent with each other,

---

* Least-squares fitting does not similarly reduce the power calibration uncertainty, since it is not random, i.e., it is assumed to have the same sign at all data points.

i.e., both 2-loop values are approximately the same and the ratio of the two- to three-loop values is ~ 1.38, in good agreement with the predicted ratio of 1.41 (II. C).

b. The static power coefficient results are in agreement, within the limits of experimental error, with the dynamic oscillator rod feedback measurements obtained under similar power and flow conditions and extrapolated to zero cps frequency.[16]

c. The two- and three-loop values from the first three measurements are about 19% smaller than the predicted values of -0.346 ¢/Mwt and -0.246 ¢/Mwt, respectively (II. C). However, the fact that the power-reactivity feedback is apparently somewhat smaller than originally anticipated was not unexpected, since the isothermal temperature coefficient value measured in the low-power test program was also found to be smaller than originally predicted, but only by 12% (-0.82 ih/F versus -0/93 ih/F, respectively[12]). Considering the greater degree of complexity in the power coefficient calculations, as compared to the temperature coefficient calculations, the agreement here was felt to be satisfactory.

d. The power coefficient value obtained in the fourth measurement made at 100 Mwt 3-loop operation (-0.162 ¢/Mwt) appears to be inconsistent with the first three values, i.e., it is 20% smaller than the other three-loop values (34% smaller than originally predicted), and the two-loop values are 1.7 times larger. The discrepancy, however, was still within the ± 25% uncertainty limits of the measurements and no particular attention was paid to it at the time.

e. Although it first appeared that the Fermi reactor power coefficient was exhibiting a hysteresis effect similar to that observed in EBR-II, it now appears that with reliable inlet temperature data, there is no hysteresis and the power coefficients for power ascent and descent are the same.

## C. FINAL DATA ANALYSES

The power coefficient results reported in Table VII were seen to have large uncertainties. This was mainly because of the power and flowmeter calibration uncertainties discussed previously and also because of the fact that the measurements were made under varying test flow conditions. However, in lieu of heat balance data, no attempt was made at the time to correct

the initial power coefficient measurements to the correct values of power and flow. This was done after completion of detailed heat balance measurements when more accurate calibration data became available. A description of these corrections is given below.

1. Correction Factors for Power and Flow

From the heat balance analyses[6, 17] correction factors for the Keithley power indicator and flowmeter readings were obtained. The results were based on the average of five different heat balances made with both 2-loop and 3-loop flow and made at power levels ranging from 67 Mwt to 100 Mwt. By use of these data, the power and flows could be determined to an estimated accuracy of $\pm$ 5%. The power correction factor obtained was:

$$P_k/P_{hb} = 1.12 \tag{1}$$

where $P_k$ = Keithley power

$P_{hb}$ = heat balance (or actual) power

Similarly, the flowmeter correction factors obtained for each loop (sum of 14-inch and 6-inch line flows) were:

$$\text{Loop 1} \quad F_a/F_m = 0.889 \tag{2}$$

$$\text{Loop 2} \quad F_a/F_m = 0.913 \tag{3}$$

$$\text{Loop 3} \quad F_a/F_m = 0.845 \tag{4}$$

where $F_a$ = actual flow

$F_m$ = meter flow

The initial power coefficient values in Table VII were corrected for the power error merely by multiplying the values given by the correction factor in Equation (1). These corrections, which accounted for the fact that the Keithley power indicator was apparently reading 12% too high, are shown in Table VIII. However, to correct the initial power coefficient values to the correct values of flow was not as straightforward. This required that the power coefficient variation with flow be known, i.e., although the metered flows for the various individual loops during each measurement could be multiplied by the correction factors given in Equations (2) through (4) to obtain the actual total test flows (Table VIII), the derivative of the power coefficient with respect to flow had to be known to correct the initial power coefficients for the difference between these flows and the programmed two- or three-loop flows. This derivative is defined as the flow coefficient, and its derivation from the experimental data is explained below.

TABLE VIII - INITIAL DATA CORRECTED FOR POWER AND FLOW

| Test Description | Loop No. | Sum of 14-inch and 6-inch Line Flows, $10^6$ lb/hr: Meter[a] | Correction Factor | Actual | Desired Programmed Flow | Initial Power Coefficient, ¢/Mwt[b] | Power Calibration Correction Factor | Initial Power Coefficient Corrected for Power, ¢/Mwt | Flow Correction, ¢/Mwt | Final Corrected Power Coefficient, ¢/Mwt | Extrapolated 2-Loop to 3-Loop or 3-Loop to 2-Loop Power Coefficient, ¢/Mwt |
|---|---|---|---|---|---|---|---|---|---|---|---|
| Measurement No. 1 13 Mwt 2 Loops | 1 | 3.04 | 0.889 | 2.70 | 2.95 | | | | | | |
| | 2 | -0.20 | 0.913 | -0.18 | 0 | -0.269 | 1.12 | -0.301 | +0.054 | -0.247 | -0.167 |
| | 3 | 2.79 | 0.845 | 2.36 | 2.95 | (±25%) | | (±23%) | | (±13%) | (3 Loops) |
| | Total | 5.63 | - | 4.88 | 5.90 | | | | | | |
| Measurement No. 2 20 Mwt 3 Loops | 1 | 3.00 | 0.889 | 2.67 | 2.95 | | | | | | |
| | 2 | 3.00 | 0.913 | 2.74 | 2.95 | -0.200 | 1.12 | -0.224 | +0.020 | -0.204 | -0.302 |
| | 3 | 2.95 | 0.845 | 2.49 | 2.95 | (±25%) | | (±23%) | | (±13%) | (2 Loops) |
| | Total | 8.95 | - | 7.90 | 8.85 | | | | | | |
| Measurement No. 3 67 Mwt 2 Loops | 1 | 2.75 | 0.889 | 2.44 | 2.95 | | | | | | |
| | 2 | 2.83 | 0.913 | 2.58 | 2.95 | -0.283 | 1.12 | -0.317 | +0.054 | -0.263 | -0.178 |
| | 3 | -0.16 | 0.845 | -0.14 | 0 | (±23%) | | (±20%) | | (±7-1/2%) | (3 Loops) |
| | Total | 5.42 | - | 4.88 | 5.90 | | | | | | |
| Measurement No. 4 100 Mwt 3 Loops | 1 | 3.12 | 0.889 | 2.77 | 2.95 | | | | | | |
| | 2 | 3.17 | 0.913 | 2.89 | 2.95 | -0.162 | 1.12 | -0.181 | +0.007 | -0.174 | -0.258 |
| | 3 | 3.32 | 0.845 | 2.81 | 2.95 | (±23%) | | (±20%) | | (±7-1/2%) | (2 Loops) |
| | Total | 9.61 | - | 8.47 | 8.85 | | | | | | |

a. See Tables III and IV
b. Table VII

## 2. Relationship Between Power Coefficient and Flow

Theoretical considerations[1] show that the power coefficient may be a represented by the sum of a constant term, which is independent of flow, and a second term that varies inversely as flow,

$$PC = A + \frac{B_o F_o}{F} \tag{5}$$

where

PC = power coefficient, ¢/Mwt

A = constant term, ¢/Mwt

F = total flow, lb/hr

$F_o$ = arbitrary reference flow, lb/hr

$B_o$ = value of second term at $F = F_o$, ¢/Mwt

In the Fermi reactor most of the reactivity feedback due to power changes comes from components (II. C) that can be related to changes in either the average fuel temperature, average core coolant temperature, or average exit coolant temperature (the inlet temperature is assumed to remain constant). On this basis, the terms A and $B_o$ in Equation (5) can be shown to have the following representation:[15]

$$A = \left(\frac{d\rho}{dT_{FA}}\right)\left(\overline{\frac{d\Delta T_{F-C}}{dP}}\right) \tag{6}$$

$$B_o = \left(\frac{d\rho}{dT_{FA}} + \frac{d\rho}{dT_{CA}}\right)\left(\frac{dT_{CA}}{dP}\right)^{F_o} + \left(\frac{d\rho}{dT_{CE}}\right)\left(\frac{dT_{CE}}{dP}\right)^{F_o} \tag{7}$$

or

$$B_o = \left(\frac{d\rho}{dT_{FA}} + \frac{d\rho}{dT_{CA}} + \frac{2d\rho}{dT_{CE}}\right)\left(\frac{dT_{CA}}{dP}\right)^{F_o} \tag{8}$$

In these equations, the three $(d\rho/dT)$ terms represent the at-power temperature coefficients with respect to the average fuel ($T_{FA}$), average core coolant ($T_{CA}$), and average exit coolant ($T_{CE}$) base tempera tures, respectively. The two $(dT/dP)^{F_o}$ terms represent the derivatives of the latter two average base temperatures with respect to power evaluated at the arbitrary reference flow $F = F_o$. In addition, the derivative of the aver-

age fuel temperature with respect to power at $F = F_o$ has been broken up into its two components

$$\left(\frac{dT_{FA}}{dP}\right)^{F_o} = \left(\frac{dT_{CA}}{dP}\right)^{F_o} + \frac{\overline{d\Delta T_{F-C}}}{dP}$$

where the first term varies inversely with flow and the second term, the average temperature rise from fuel to clad, is flow-independent. Equation (8) was obtained from Equation (7) using the relationship $(dT_{CE}/dP)^{F_o} = (2dT_{CA}/dP)^{F_o}$.

The power- and flow-corrected data in Table VIII were used to find the constants A and $B_o$ of Equation (5). To do this, the arbitrary reference flow $F_o$ was first set equal to the programmed 3-loop, 14-inch plus 6-inch line flow, $8.85 \times 10^6$ lb/hr ($2.95 \times 10^6$ lb/hr/loop). Two simultaneous equations of the form of Equation (5) were then set up, each of which utilized the power-corrected power coefficient values PC and actual total flows F from two different measurements. From these, it was possible to obtain the values for A and $B_o$.

The main question in making the analysis was deciding which two sets of corrected power coefficient and flow values should be used from Table VIII. Six possibilities existed: Either the two 2-loop measurements could be compared with each other, the two 3-loop measurements similarly compared, or else each 2-loop measurement could be compared to each 3-loop measurement. However, because the actual total flow was the same in both two-loop measurements (Table VIII), only three meaningful comparisons existed -- comparison of the two 3-loop measurements or comparison of each 3-loop measurement with the two-loop average measurement.

In addition to these limitations, it will also be recalled (V.B.4) that, based on the initial power coefficient analyses, one 3-loop measurement appeared peculiar and inconsistent with the other three measurements. Therefore, to avoid use of bad data in the flow coefficient calculations, this point was investigated further, using the power- and flow-corrected data given in Table VIII. The following observations were made:

a. Both 2-loop measurements are consistent, i.e., with the same flows the measured power coefficients differ by only 5%.

b. When the 2-loop corrected power coefficients and flows are compared with those from the 20 Mwt 3-loop measurement, the following ratios are found:

$$\frac{\text{2-loop PC (Avg)}}{\text{3-loop PC (20 Mwt)}} = \frac{-0.309\ ¢/\text{Mwt}}{-0.224\ ¢/\text{Mwt}} = 1.38 \qquad (9)$$

$$\frac{\text{3-loop flow (20 Mwt)}}{\text{2-loop flow}} = \frac{7.90 \times 10^6\ \text{lb/hr}}{4.88 \times 10^6\ \text{lb/hr}} = 1.62 \qquad (10)$$

Since the predicted power coefficient ratio was 1.41 for a flow ratio of 1.50 (II. C), these results indicate a flow-independent power coefficient component that is considerably larger than the calculated value.

c. When the 2-loop corrected power coefficients and flows are similarly compared to the 100 Mwt 3-loop values, these ratios are found:

$$\frac{\text{2-loop PC (Avg)}}{\text{3-loop PC (100 Mwt)}} = \frac{-0.309\ ¢/\text{Mwt}}{-0.181\ ¢/\text{Mwt}} = 1.71 \qquad (11)$$

$$\frac{\text{3-loop flow (100 Mwt)}}{\text{2-loop flow}} = \frac{8.47 \times 10^6\ \text{lb/hr}}{4.88 \times 10^6\ \text{lb/hr}} = 1.73 \qquad (12)$$

These results indicate a flow-independent power coefficient component considerably smaller (almost zero) than originally predicted.

d. Similarly, when the two sets of 3-loop data are compared, the ratios are

$$\frac{\text{3-loop PC (20 Mwt)}}{\text{3-loop PC (100 Mwt)}} = \frac{-0.224\ ¢/\text{Mwt}}{-0.181\ ¢/\text{Mwt}} = 1.24 \qquad (13)$$

$$\frac{\text{3-loop flow (100 Mwt)}}{\text{3-loop flow (20 Mwt)}} = \frac{8.47 \times 10^6\ \text{lb/hr}}{7.90 \times 10^6\ \text{lb/hr}} = 1.07 \qquad (14)$$

These results are not consistent with the results of either item b or c. In fact, they indicate a flow-independent power coefficient component which is positive and/or a flow component for which the inverse flow effect is greater than unity. The first possibility is very unlikely and the second is physically impossible. Therefore, it can be concluded that one of the 3-loop measurements must be in error regarding its power coefficient value and/or flow value.

On the basis of the above observations, it was clear that the flow coefficient calculations should not be made by intercomparison of the data from the two 3-loop measurements. However, it was not immediately clear which set of 3-loop data was the most accurate and should be compared to the 2-loop data to obtain the best estimate of the flow coefficient. If the 20 Mwt data were used, a flow dependence smaller than originally predicted would be obtained; whereas, a comparison using the 100 Mwt data would give a flow dependence larger than predicted. It was finally decided that the 100 Mwt 3-loop data should be compared with the 2-loop data as done in item c. This somewhat arbitrary decision was based primarily on the fact that revised power coefficient calculations (Section V) indicate a smaller flow-independent feedback component (mainly the fuel pin axial expansion component) than originally calculated. Some of the unofficial power coefficient measurements (see Appendix A) also suggest this fact. However, it is doubtful whether the effect is actually as small as indicated in item c.*

When two simultaneous equations of the form of Equation (5) are set up, using the corrected power coefficient and flow data given in item c and using an arbitrary reference flow $F_o = 8.85 \times 10^6$ lb/hr, the following values of A and $B_o$ are obtained:

$$A = -0.0070 \text{ ¢/Mwt}$$
$$B_o = -0.1670 \text{ ¢/Mwt}$$

or

$$PC = -0.0070 - \frac{0.1670 F_o}{F} \text{ ¢/Mwt} \qquad (15)$$

where

$$F_o = 8.85 \times 10^6 \text{ lb/hr}$$

To correct the power-corrected power coefficient values given in Table VIII to the programmed flow values, the derivative of the power coefficient with respect to flow had to be known. From Equations (5) and (15),

$$\frac{d(PC)}{dF} = - \frac{B_o F_o}{F^2} = \frac{1.48 \times 10^6}{F^2} \text{ ¢/Mwt/lb/hr} \qquad (16)$$

---

* The preliminary conclusion reached in Sec. IV.B.4 was that the 20 Mwt 3-loop results appeared correct and the 100 Mwt 3-loop results were inconsistent. However, after making the power and flow corrections, both 3-loop results are inconsistent with the 2-loop results, when compared to the original predictions. Therefore, no definite conclusion can be reached as to which is actually correct.

### 3. Final Corrected Power Coefficient Values

The power-corrected power coefficient values for the four measurements given in Table VIII were corrected to the desired programmed flow conditions, using the actual total flows and Equation (16). To make the flow corrections, the flow coefficient given by Equation (16) was evaluated for both the actual test flow and desired programmed flow in each case, and the average of the two slopes used for the flow correction, i.e.,

$$\text{Flow Correction} = \left(\frac{\overline{d(PC)}}{dF}\right)\left(F_2 - F_1\right) \text{ ¢/Mwt} \qquad (17)$$

where

$$\overline{dPC/dF} = \frac{(dPC/dF)^{F_1} + (dPC/dF)^{F_2}}{2}$$

$F_2$ = programmed flow, lb/hr

$F_1$ = actual test flow, lb/hr

The flow corrections found were added to the power-corrected power coefficient values to obtain the final corrected power coefficient values.* The flow corrections and final power coefficient values are given in Table VIII.

In a similar manner, it was possible to obtain extrapolated 3-loop power coefficients from the 2-loop values and vice versa. These data, shown in Table VIII, were also used for consistency checks.

The estimated uncertainties in the measurements after making the power and flow corrections are given in Table VIII and as seen they are considerably smaller than the original uncertainties. The revised error estimates were made in the same manner described earlier (IV.B.3) but are based on estimated uncertainties of only $\pm$ 5% in both the corrected power and flow values. The reactivity measurement uncertainties were not affected by the corrections made and remained the same as before.

---

* When making the flow corrections it is assumed that the flow division between the 14-inch and 6-inch lines in each loop during the measurements was as programmed (87% of the total flow through the 14-inch line). Although this was not always true (see Tables III and IV), the differences were small enough that the effect on the final power coefficient values was negligible and could be neglected.

## 4. Final Conclusions

On the basis of the power- and flow-corrected results, a number of conclusions can be made. They are summarized below:

a. The power coefficient values obtained in the three measurements made at 13 Mwt 2-loop operation (-0.247 ¢/Mwt), 67 Mwt 2-loop operation (-0.263 ¢/Mwt), and 100 Mwt 3-loops operation (-0.174 ¢/Mwt) are consistent with each other; i.e., both 2-loop values are essentially the same and, using the measured flow dependence, the 2-loop values extrapolate to the 3-loop value and vice versa.

b. The 2-loop and 3-loop power coefficient values from these three measurements are all about 28% smaller than the originally predicted values of -0.346 ¢/Mwt and -0.246 ¢/Mwt, respectively (II.C.). Although the power-reactivity feedback discrepancy is larger than the isothermal temperature coefficient discrepancy of 12% discussed earlier, it now appears that both discrepancies can be explained by more recent calculations (V).

c. The flow-dependence of the power coefficient obtained from these three measurements is surprising in that it shows very little feedback independent of flow, i.e., the constant term A in Equation (15) due to the temperature rise from clad to fuel is only 4% of the total feedback with 3-loop flow. Based on the originally calculated 3-loop and 2-loop power coefficients (II.C.), a similar analysis for the predicted power coefficient variation with flow gives

$$PC = -0.046 - \frac{0.200\ F_o}{F}\ ¢/\text{Mwt} \qquad (18)$$

where

$$F_o = 8.85 \times 10^6\ \text{lb/hr}$$

In this case, therefore, the constant feedback term constitutes about 18-1/2% of the total 3-loop feedback. Although there is reason to believe that the flow independent feedback is smaller than originally predicted, it is doubtful whether it is actually as small as given by Equation (15). The $\pm$ 7-1/2% uncertainty in the final corrected power coefficient values is sufficiently large to account for most of the difference seen.

d. The power coefficient value obtained in the measurement made at 20 Mwt 3-loop operation (-0.204 ¢/Mwt), appears to be inconsistent with the other three values, i.e., it is 17% larger than the other 3-loop value (which is outside the uncertainty limits of the corrected measurements) and its extrapolated 3-loop to 2-loop value does not agree with the 2-loop measurements. No adequate explanation for this inconsistency presently exists. It should be realized, however, that the inconsistency is actually the result of the rather arbitrary flow-dependence correction used in IV. C. 2. If the A and $B_o$ terms in Equation (5) had been found using the smaller flow dependence indicated by item b in IV. C. 2, then the 100 Mwt 3-loop power- and flow-corrected power coefficient value would have instead appeared inconsistent in relationship to the other measurements.

# V. REVISED TEMPERATURE COEFFICIENT AND POWER COEFFICIENT CALCULATIONS

The isothermal temperature coefficient and power coefficient values originally calculated for the Fermi reactor are shown in Table I. These early calculations were made before the reactor design was completely finalized. Although the final reactor design contained several significant changes, such as a reduction in primary sodium flow, the addition of subassembly bypass flow, and others, the effect of these changes on the original feedback calculations had never been calculated in detail.

However, as seen the experimental measurements made for the reactor have resulted in actual temperature and power coefficients somewhat smaller than originally predicted. Because of the importance of these measurements, the original calculations have therefore been reviewed and new temperature and power coefficients calculated in an attempt to explain the discrepancies.[18] The revised estimates, although still not finalized, appear to explain adequately the observed discrepancies.

## A. BASIS OF NEW PREDICTIONS

### 1. Isothermal Temperature Coefficient Calculations

All components of the isothermal temperature coefficient, except the Doppler component, have values which depend on the distributed worths of the fuel, coolant and structural materials, and the material thermal expansion coefficients. The primary basis for the revised isothermal temperature coefficient predictions was the use of recently calculated two-dimensional distributed worths, using the CRAM diffusion theory code.[19] These recent calculations agree very well with the worths measured during the low-power nuclear test program.[20, 21] They were used for the revised predictions rather than the measured worths because of their greater flexibility in the calculations. It should be mentioned that the calculated worths were obtained for the core size which existed during the low-power worth measurements. This size was slightly smaller ($\sim$ 4%) than the core size at the time of the temperature and power coefficient measurements, the effect on the accuracy of the revised predictions is believed to be small.

Besides the use of new two-dimensional calculated material worths, a better calculational model than that used originally was used for the revised isothermal radial core expansion and axial fuel pin expansion calculations. The Doppler component was obtained using an updated set of nuclear constants and also a better calculational technique.[22] No changes in any of the thermal expansion coefficients were made.

## 2. Power Coefficient Calculations

Each component of the power coefficient has a value determined by the product of an at-power temperature coefficient, defined with respect to a selected average base temperature, and the derivative of the average base temperature with respect to power. The at-power temperature coefficients in turn depend on the isothermal temperature coefficient values, which are dependent on the distributed worths appropriately weighted by the temperature distribution in the reactor with respect to the selected base temperature.

The revised power coefficient predictions therefore used the same CRAM two-dimensional calculated worths and better calculation models for the radial core expansion, axial fuel pin expansion, and Doppler components than were used in the revised isothermal temperature coefficient predictions. Also, the same average base temperatures as used in the original power coefficient analyses were used and, except for one component, the same temperature distributions were assumed, i.e., the ratio of the at-power to isothermal temperature coefficients for each component in the revised calculations was kept the same. The important exception was the change made in the temperature at the subassembly spacer pads relative to the average sodium temperature, which resulted from including the effect of bypass flow. This caused a reduction in the at-power radial core expansion temperature coefficient compared to the earlier calculations.

The only change made in the derivatives of the average base temperatures with respect to power was an over-all increase in their values to account for the primary flow reduction made since the time of the original analyses. The flow was reduced so as to increase the core coolant $\Delta T$ from 250 F to 270 F, i.e., a 7-1/2% reduction. This change affected the power coefficient components tied to core sodium temperature more than those tied to average fuel temperature; however, because of the flow-independent term of the latter the temperature distribution in the reactor is also slightly changed by reduced flow. Nevertheless, the effect on the at-power temperature coefficients is small and was neglected in the analyses.

# B. RESULTS

The revised isothermal temperature coefficient predictions and 3-loop full flow power coefficient predictions are summarized in Tables IX and X, respectively. The original predictions and the measured values are also given for comparison. The bases for the new calculations are given in the last column on the right in the tables for each component. As can be seen, no attempt was made to revise some of the smaller and relatively unimportant isothermal temperature coefficient components.

TABLE IX - REVISED ISOTHERMAL TEMPERATURE COEFFICIENT PREDICTIONS

| Component | Isothermal Temperature Coefficient Value, $10^{-6}$ $\Delta k/k/C$ Original | Revised | Basis of Revision |
|---|---|---|---|
| Core | | | |
| Sodium Expansion | -4.44 | -7.45 | CRAM Sodium Worth |
| Fuel Pin Radial Expansion | -0.36 | -0.60 | CRAM Sodium Worth |
| Fuel Pin Axial Expansion | -5.80 | -3.69 | CRAM Fuel Worths and Better Model |
| Doppler | -2.50 | -1.70 | New Data and Better Calculation Technique |
| Bowing | - | - | --- |
| Lower Support Expansion | -1.47 | -0.77 | CRAM Worths and Better Model |
| Subassembly Radial Expansion | -11.33 | -6.82 | CRAM Worths and Better Model |
| Holddown Plate Expansion | +0.02 | +0.02 | --- |
| Inner Radial Blanket (IRB) | | | |
| Sodium Expansion | -1.70 | -2.14 | CRAM Sodium Worth |
| Pin Expansion | -0.24 | -0.24 | --- |
| Displacement Due to Core Radial Expansion | -0.67 | -1.34 | CRAM Worths and Better Model |
| Displacement Due to Hold-Down Mechanism Expansion | -0.28 | -0.28 | --- |
| Axial Blanket (AB) | | | |
| Sodium Expansion | -5.22 | -4.02 | CRAM Sodium Worth |
| Axial Expansion | -0.09 | -0.09 | --- |
| Radial Expansion | -0.06 | -0.06 | --- |
| Expansion Due to Holddown Mechanism Expansion | -0.42 | -0.42 | --- |
| TOTALS | -34.56 | -29.60 | |
| | (-0.926 ih/F) | (-0.795 ih/F) | |

Measured Value = -0.82 ih/F

TABLE X - REVISED THREE-LOOP POWER COEFFICIENT PREDICTIONS

| Component | At-Power Temperature Coefficient, $10^{-6}$ Δk/k/C Original | Revised | Power Coefficient, ¢/Mwt Original | Revised | Base Temperature | Basis of Revision |
|---|---|---|---|---|---|---|
| Core | | | | | | |
| Sodium Expansion | -4.16 | -6.98 | -0.0209 | -0.0381 | Avg. Na | Reduced Flow, CRAM Sodium Worth |
| Fuel Pin Radial Expansion | -0.33 | -0.55 | -0.0030 | -0.0053 | Avg. Fuel | Reduced Flow, CRAM Sodium Worth |
| Fuel Pin Axial Expansion | -6.96 | -4.43 | -0.0650 | -0.0432 | Avg. Fuel | Reduced Flow, CRAM Fuel Worths, Better Model |
| Doppler | -2.47 to -1.68 | -1.66 to -1.13 | -0.0189 (Avg.) | -0.0133 | Fuel | Reduced Flow, New Data and Calculation Techniques |
| Bowing | +0.44 | +0.27 | +0.0023 | +0.0015 | Avg. Na | Reduced Flow, Better Model, CRAM Fuel Worths |
| Lower Support Expansion | - | - | - | - | Inlet Na | ---------- |
| Subassembly Radial Expansion | -17.96 | -7.68 Δ | -0.0942 | -0.0440 | Avg. Na | Reduced Flow, Bypass Flow, CRAM Worths, Better Model |
| Holddown Plate Expansion | +0.02 | +0.02 | +0.0002 | +0.0002 | Exit Na | Reduced Flow |
| Inner Radial Blanket (IRB) | | | | | | |
| Sodium Expansion | -1.70 | -2.14 | -0.0089 | -0.0087 | Avg. IRB Na | Reduced Flow, CRAM Sodium Worth |
| Pin Expansion | -0.24 | -0.24 | -0.0022 | -0.0023 | Avg. IRB Alloy | Reduced Flow |
| Displacement Due to Core Radial Expansion | -0.63 | -0.95 | -0.0033 | -0.0054 | Avg. Na | Reduced Flow, Bypass Flow, CRAM Worths, Better Model |
| Displacement Due to Holddown Mechanism Expansion | -0.14 | -0.14 | -0.0015 | -0.0015 | Exit Na | Reduced Flow |
| Axial Blanket (AB) | | | | | | |
| Sodium Expansion | -2.61 | -2.01 | -0.0274 | -0.0229 | Exit Na | Reduced Flow, CRAM Sodium Worth |
| Axial Expansion | -0.04 | -0.04 | -0.0007 | -0.0007 | Avg. UAB Alloy | Reduced Flow |
| Radial Expansion | -0.06 | -0.06 | -0.0002 | -0.0003 | Avg. Na | Reduced Flow |
| Expansion Due to Holddown Mechanism Expansion | -0.21 | -0.21 | -0.0020 | -0.0024 | Exit Na | Reduced Flow |
| | | TOTALS | -0.2458 | -0.1864 | | |

Measured Value = -0.174 ¢/Mwt

Four important changes in the revised temperature and power coefficients are evident in Tables IX and X.

1. There is a large increase in the size of those components which depend upon core sodium worth.

2. There is a large decrease in the core fuel pin axial expansion component, which tends to reduce the flow independent component of the power coefficient.

3. There is a large decrease in the core radial expansion components, which is more pronounced for the power coefficient than the temperature coefficient because of the bypass flow effect in the former case.

4. The revised temperature and power coefficient predictions are in considerably better agreement with the measured values than the original predictions.

## VI. DISCUSSION

The Fermi reactor power coefficient measurements were not as straightforward as originally anticipated. Some difficulty was encountered in making the measurements and interpreting the data. Data corrections to account for power drift, burnup, and inlet temperature variations were needed; even after making these corrections, the early results had large uncertainties due to power and flowmeter calibration uncertainties.

In addition, the early results exhibited an apparent hysteresis effect in the power ascent and power descent modes of operation. The hysteresis effect disappeared after more accurate inlet temperature information was obtained, and the measurement errors were reduced to reasonable values when more accurate power and flow calibration data became available from heat balance measurements. Nevertheless, the 20 Mwt 3-loop power coefficient results still look inconsistent when compared to the other three measurements. No adequate explanation has been found for this. The results of the measurements also indicate that the flow-independent feedback portion of the total power coefficient is considerably smaller than originally predicted. Furthermore, the 2-loop and 3-loop coefficients were found to be on the average about 28% smaller than originally predicted. More refined calculations recently made apparently explain these two latter discrepancies, as well as an earlier discrepancy found between the measured and predicted isothermal temperature coefficient values.

In conclusion, it is felt that from the results of this test sufficient knowledge has been gained of the reactor power-reactivity feedback behavior and flow effects to allow its operation in an efficient and safe manner.

## REFERENCES


1. "Enrico Fermi Hazards Summary Report and Technical Information," Volumes 1 through 9, as amended, Power Reactor Development Company, March 1964.

2. Bethe, H. A., "On the Doppler Effect in Fast Reactors," APDA-119, 1957.

3. Branyan, C. E., "Core A Critical Studies for the Enrico Fermi Atomic Power Plant on ZPR-III," ANL-6629, 1962.

4. Wilber, H. A., "Power Coefficient of Reactivity," Nuclear Test Procedure No. 22, APDA, 1963.

5. Mueller, R. E., et al, "Enrico Fermi Nuclear Test Program," APDA-305, to be published.

6. Callen, R. C., "Thermal Measurement of Power in the Enrico Fermi Reactor," APDA-NTS report to be published.

7. Page, E. M., and Horne, R. E., "Preliminary Evaluation of NTP-2, "Absolute Power Calibration," APDA Internal Memorandum P-63-383, 1963.

8. Page, E. M., and Horne, R. E., "Flux Mapping Measurements to Determine the Location of the Permanent Detectors in the Enrico Fermi Reactor," APDA-NTS-8, 1966.

9. Mueller, R. E., and Branyan, C. E., "Preliminary Evaluation of NTP-6, Calibration of Shim and Regulating Rods," APDA Internal Memorandum P-64-65, 1964.

10. Horne, R. E., "General Reactivity Measurements," Nuclear Test Procedure No. 14, APDA, 1962.

11. Mueller, R. E., "Summary of Base Reactivity Data Obtained Since Start of High Power Tests," APDA Internal Memorandum P-66-418, 1966.

12. Wilber, H. A., et al, "Measurement of the Isothermal Temperature Coefficient of Reactivity of the Enrico Fermi Reactor," APDA-NTS-5, 1965.

13. Novick, M., et al, "EBR-I and EBR-II Operating Experience," ANS-100, Paper No. 3 of Session 1, 1965.

14. Mueller, R. E., "Results of Power Coefficient Measurements Made at 13 Mwt and 20 Mwt," APDA Internal Memorandum P-66-123, 1966.

15. Mueller, R. E., "Summary of Power Coefficient Data Obtained Through the 100 Mwt Tests," APDA Internal Memorandum P-66-381, 1966.

16. Klickman, A. E., "Oscillator Tests in the Enrico Fermi Reactor," APDA-NTS-11, 1967.

17. Allgeier, H. J., and Callen, R. C., "Enrico Fermi Heat Balance Measurements," APDA Internal Memorandum P-66-306, 1966.

18. Mueller, R. E., "Revised Isothermal Temperature Coefficient and Power Coefficient Predictions," APDA Internal Memorandum P-66-324, 1966.

19. Hassitt, A., "A Computer Program to Solve the Multigroup Diffusion Equations," TRG Report 229 (R), 1962.

20. Ball, G. L., et al, "Worth Measurements of Core and Blanket Subassembly Materials in the Enrico Fermi Reactor," APDA-NTS-6, 1965.

21. Segal, B. M., and Horne, R. E., "Measurement of Sodium Worth in the Enrico Fermi Reactor," APDA-NTS-7, 1966.

22. Nicholson, R. B., "The Doppler Effect in Fast Neutron Reactors," APDA-139, 1960.

# APPENDIX A: UNOFFICIAL POWER COEFFICIENT MEASUREMENTS

## INTRODUCTION

In addition to the power coefficient values obtained in the official power coefficient measurements, numerous unofficial power coefficient measurements were made throughout the course of the high power nuclear testing. Such data were obtained practically every time the reactor was brought up to power. It is the purpose of this Appendix to report these data.

In contrast to the accurate and detailed measurements made in the official power coefficient tests, the unofficial data were obtained in a rather haphazard manner. For example, data were usually taken only at zero power and full test power. Often only approximate power levels were recorded, and in most cases the temperature reading of only one inlet thermocouple was recorded. Furthermore, temperatures were not always recorded at all power levels, and sometimes flow data were not recorded. In addition, care was not always taken to ensure that the reactor was in equilibrium before making the measurements; the position of the oscillator rod was seldom recorded; and usually no data for burnup corrections were taken.

Consequently, in many cases the unofficial data obtained were insufficient for meaningful analysis. In other cases, gaps in the data had to be filled from information obtained from the operator's log books, from plant charts and records, and by estimates. In all cases the probable error of the measurements was quite large ($\sim \pm$ 10% minimum and $\pm$ 33% maximum). The maximum uncertainty occurred in the relatively low power measurements (up to $\sim$ 20 Mwt). At higher power levels, the accuracy improved considerably because the rod position, temperature, and other uncertainties were relatively less important in comparison with the total reactivity change being measured.

In spite of the rather large uncertainty in the unofficial measurements, they are given with the intent that, hopefully, by comparison with the official measurements, they can be used to give an indication of any dramatic changes which may have occurred in the power coefficient during testing; i.e., perhaps they might help to explain the 3-loop power coefficient anomaly seen in the official measurements or give an indication of other possible power reactivity feedback anomalies.

## RESULTS OF MEASUREMENTS

Descriptions of the unofficial 2-loop and 3-loop power coefficient measurements and their results are given in Tables A.I and A.II, respectively. The official measurement data are also given in these tables for comparison. As stated previously, the data used in the unofficial measurement analyses were obtained from various sources, but primarily from the author's notes, the plant operator log books, and from plant charts and records. The data were analyzed in the same manner as described in the main text. All power coefficients have been adjusted to the correct values of power and flow. However, for simplification the flow correction was made using the assumption that the power coefficient varies inversely as flow. This is very nearly the same conclusion as reached from analysis of the official measurements in the text. The last column in each table gives some pertinent comments concerning various aspects of the measurements.

## DISCUSSION

The results shown in Tables A.I and A.II have not been analyzed in detail; however, a few preliminary observations have been made.

Concerning the 2-loop data, three measurements seem to be inconsistent with the others; i.e., the power coefficients obtained on January 12, 1966 and January 18, 1966 appear to be somewhat smaller than the consensus value of $\sim -0.260$ ¢/Mwt, whereas the August 25, 1966 value is considerably larger. The two smaller values were measured at very low power, however, and their discrepancy is within the range of values given by the maximum experimental uncertainty of $\pm$ 33%. In particular, the inlet temperature changes associated with these measurements could be in error. A change of only a few degrees in these data, i.e., an additional inlet temperature change of -2F, would account for the discrepancy seen.

The extraordinarily large 2-loop power coefficient found on August 25, 1966 can be largely explained, on the other hand, by the fact that this was the date on which the blanket throttle valve was changed to allow a larger than normal portion of the total flow to pass through the blanket and a smaller than normal portion through the core. The footnote in Table A.I shows that if the flow correction is made on the basis of core flow only in this case, then the agreement is much better.

The preliminary conclusion reached from review of the 2-loop power coefficient data is that no dramatic 2-loop feedback anomalies occurred during the high power test period.

TABLE A.I - TWO-LOOP MEASUREMENTS

| | | OPERATING CONDITIONS* | | | | | |
|---|---|---|---|---|---|---|---|
| Date | Type | Operating Loops | Actual Flow, $10^6$ lb/hr | Connected Power Range, Mwt | Inlet Temperature Change, F | Measured Power Coefficient, Corrected For Power And Flow, ¢/Mwt* | Comments |
| 1/10/66 | Unofficial | 1 & 3 | 5.22 | 0 to 5.8 | -1.0 | -0.287 | |
| 1/12/66 | Unofficial | 1 & 3 | 5.05 | 0 to 11.9 | -3.3 | -0.206 | Inlet temperature change looks small compared to 1/13/66 data. |
| 1/13/66 | Official | 1 & 3 | 4.88 | 0 to 11.9 | -6.5 | -0.247 | |
| 1/18/66 | Unofficial | 1 & 3 | 5.05 | 0 to 11.6 | +1.5 | -0.210 | Flow had to be estimated here. First time sign of inlet temperature change was positive as programmed. |
| 4/18/66 | Unofficial | 2 & 3 | 5.27 | 0 to 8.9 | +2.0 | -0.258 | Flow and inlet temperature change both were estimated here. |
| 6/23/66 | Unofficial | 1 & 2 | 4.64 | 0 to 59.8 | +23.0 | -0.265 | More accurate than usual data taken here because this run was an aborted official measurement. |
| 6/24/66 | Official | 1 & 2 | 4.89 | 0 to 59.8 | +28.5 | -0.263 | |
| 7/1/66 | Unofficial | 1 & 2 | 5.89 | 0 to 65.2 | +35.5 | -0.256 | Note that the flows were adjusted exactly correct in this run. |
| 8/25/66 | Unofficial | 2 & 3 | 6.18 | 0 to 65.2 | +55.0 | -0.310** | On the day of this run the blanket throttle valve had been changed. |

* The flows given are the actual 2-loop total flows (metered flows times heat balance correction factors). Backflow in the nonoperating loop was taken into account. The power range over which the measurements were made was obtained by dividing the Keithley powers by the heat balance correction factor (1.12). The inlet temperature change over the measurement power range is given to help explain possible sources of error in the measurements. The flow correction to the programmed 14-inch plus 6-inch line 2-loop total flow of $5.9 \times 10^6$ lb/hr was made using the assumption $P\,C \propto 1/F$.

** If the flow connection for this measurement is made instead such that only the total core flow (14-inch line) agrees with the programmed 2-loop value of $5.12 \times 10^6$ lb/hr through the core, then this value becomes -0.283 ¢/Mwt.

TABLE A.II - THREE-LOOP MEASUREMENTS

| | | OPERATING CONDITIONS* | | | | | |
|---|---|---|---|---|---|---|---|
| Date | Type | Operating Loops | Actual Flow, $10^6$ lb/hr | Connected Power Range, Mwt | Inlet Temperature Change, F | Measured Power Coefficient, Corrected For Power And Flow, ¢/Mwt* | Comments |
| 1/10/66 | Unofficial | All | 8.20 | 0 to 5.4 | -1.4 | -0.206 | Flow had to be estimated here. |
| 1/28/66 | Unofficial | All | 8.28 | 0 to 17.9 | +10.0 | -0.153 | Flow had to be estimated here. Inlet temperature change looks large compared to 2/1/66 data. |
| 2/1/66 | Official | All | 7.90 | 0 to 17.9 | +0.4 | -0.204 | |
| 7/8/66 | Unofficial | All | 9.88 | 0 to 98.2 | +45.0 | -0.193 | Flows were very high. Scrammed at upper power before complete equilibrium was attained. |
| 7/11/66 | Unofficial | All | 10.05 | 0 to 98.2 | +30.0 | -0.201 | Flows were very high during this run also. |
| 7/12/66 | Official | All | 8.47 | 0 to 98.2 | +29.0 | -0.174 | |
| 8/3/66 | Unofficial | All | 7.94 | 0 to 62.5 | +20.0 | -0.176 | |
| 8/5/66 | Unofficial | All | 7.94 | 0 to 98.2 | +39.0 | -0.182 | |

* The flows given are the actual 3-loop total flows (metered flows times heat balance correction factors). The power range over which the measurements were made was obtained by dividing the Keithley powers by the heat balance correction factor (1.12). The inlet temperature change over the measurement's power range is given to help explain possible sources of error in the measurements. The flow correction to the programmed 3-loop total flow of $8.85 \times 10^6$ lb/hr was made using the assumption $P\,C \propto 1/F$.

In the case of the 3-loop power coefficient data, no clear-cut interpretation of the results in Table A.II can be made. The one particularly low result found on January 28, 1966 can probably be attributed to measurement errors, i.e., the inlet temperature change (which was taken from the hard-to-read plant charts) looks large. Again, lowering the value of this inlet temperature change a few degrees would bring this power coefficient into line with the other results.

The remaining 3-loop results (excluding the official measurement made on February 1, 1966)lie well within the experimental uncertainty range of the measurements. Therefore, one interpretation of the 3-loop results given in Table A.II could be that no change occurred in the 3-loop power coefficient, except that measured on February 1, 1966, throughout the high power test period.

Another interpretation of the data in the table could also be made: In view of the extraordinarily high value found in the official measurement on February 1, 1966, and considering the other apparently high values found in the early unofficial measurements, it could also be argued that a significant and permanent reduction in the 3-loop power coefficient occurred between July 11, 1966 and July 12, 1966. However, the data in Table A.I doesnot allow one to determine whether a similar reduction in the 2-loop power coefficient also occurred. Therefore, no clear-cut conclusions can be reached regarding this point.